



**Faculty of Engineering
Nanotechnology Department**

Nanotechnology Engineering Fourth Year Design Project Final Report

Proposal: Gene detection for personalized medicine

Project identifier: 18

This report is submitted as the interim report requirement for the NE 409 course. It has been written solely by us and has not been submitted for academic credit before (other than appendices A-E) at this or any other academic institution.

Team members:

Nube Torres (20745653)

Signature:

A blue ink signature of the name Nube Torres.

Andrea Parra (20747348)

Signature:

A black ink signature of the name Andrea Parra.

Sara Thompson (20843578)

Signature:

A black ink signature of the name Sara Thompson.

Karla Castro (20745522)

Signature:

A black ink signature of the name Karla Castro.

Consultant: Shirley Tang
E-mail: tangxw@uwaterloo.ca

April 8th, 2024

Executive Summary

The key goal of this project is to develop an affordable and user-friendly biosensor for the detection of Single Nucleotide Polymorphisms (SNPs) utilizing cyclic voltammetry to detect mutations in the CYP2C19 gene. These mutations impact the metabolism of selective serotonin reuptake inhibitors (SSRIs) used to treat different mental health disorders, thereby enhancing their treatment. This device will address the issue of invasive sample collection and expensive detection methods for SNPs by offering a compatible and non-intrusive approach to obtaining genetic information derived from saliva samples. The main aspects of this device include the deposition of a self-assembled layer (SAM) consisting of 6-Mercapto-1-hexanol (MCH) and 5' thiol and 3' biotin labeled hairpin probes targeting the mutant CYP2C19*2. After the device undergoes hybridization and incubation with the enzyme reporter HRP-streptavidin, an electron-transfer mediator solution containing TMB and H₂O₂ is introduced to the system. The signal is amplified when TMB undergoes oxidation by H₂O₂ in the presence of HRP producing a change in electrical signal. Finally, a potentiostat to generate and read the signal and a user interface that includes a streamlined App and comprehensive report to project the results have been incorporated. This biosensor will meet the primary customer requirements as the collection of saliva is non-invasive and the SNP detection method is highly specific and sensitive, which incorporated into a single device, becomes user-friendly.

Acknowledgements

We would like to express our gratitude to our supervisor, Prof. Shirley Tang, who believed in our project and has supported us in many aspects. Similarly, we would like to thank PhD. Pramod Kalambate and PhD student Pei Li, who have supported us in the development of the experiments at the Tang Nanotechnology Labs. We also thank Professor Juewen Liu for dedicating his time to helping us verify our hairpin probe design, as well as Prof. Hany Aziz, Prof. Ahmad Ghavami, Prof. Howard Siu and Prof. Mishi Groh for their invaluable support, guidance, and advice. Finally, we would like to extend our thanks to the Norman Esch Foundation for providing us with additional funding through the Normal Esch Entrepreneurship Award.

Glossary of Terms and Acronyms

Anti-DIG	Digoxigenin Antibody
AuNPs	Gold Nanoparticles
cDNA	Complementary DNA
CE	Counter Electrode
COMSOL	COMSOL Multiphysics
CV	Cyclic Voltammetry
CYP2C19	Cytochrome P450, family 2, subfamily C member 19
DIG	Digoxigenin
DLS	Dynamic Light Scattering
DPV	Differential Pulse Voltammetry
dsDNA	Double-stranded DNA
ssDNA	Single-stranded DNA
EDF	Ethyl (dimethylaminopropyl) carbodiimide (EDC) and 1-hydroxybenzotriazole
ET	Electron transfer
$Fe(CN)_6^{3-}$	Hexacyanoferrate(III)/hexacyanoferrate(IV) redox couple

GC%	Guanine and Cytosine content
HRP	Horseradish peroxidases
LFA	Lateral Flow Assay
LOB	Limit of Blank
LOD	Limit of Detection
MES	2-(N-morpholino)ethanesulfonic acid
MCH	6-Mercapto-1-hexanol
MU	11-mercaptop-1-undecanol
MUA	11-mercaptoundecanoic acid
NCBI	National Institute of Health
NGS	Next Generation Sequencing
NHS	N-Hydroxysuccinimide
PCR	Polymerase Chain Reaction
PDB	Protein Databank
PEG	Polyethylene Glycol
Rct	Charge Transfer Resistance
RE	Reference Electrode

rs ID	Reference SNP Cluster Identification Number
SAM	Self-assembled Monolayers
SEM	Scanning Electron Microscopy
SNP	Single Nucleotide Polymorphism
SPE	Screen Printed Electrode
SSRI	Selective Serotonin Reuptake Inhibitors
SWV	Square Wave Voltammetry
TMB	3,3',5,5' tetramethylbenzidine
UV/Vis	Ultraviolet-visible Spectrophotometer
WE	Working Electrode

Table of Contents

1. Introduction.....	9
1.1 Problem statement	9
1.2 High-Level Description of The Design	9
1.3 Customer Requirements	10
2. Discussion	13
2.1 Design Choices	15
2.2 Design Verification.....	17
2.2.1 Design Verification Outline	17
2.2.2 Analysis of Verification Data	17
2.2.3 Deviations from Verification Plan.....	21
2.3 Prototype Construction	22
2.4 Test Results.....	24
2.4.1 Primary Requirements	25
2.4.2 Secondary Requirements	31
2.5 Deviations/Shortfalls.....	36
2.5.1 Opting Out of Gold Nanoparticles (AuNPs) on Carbon Electrodes.....	36
2.5.2 Changes in protocol for MCH	37
2.5.3 Failure of Mismatch 2	37
3. Summary.....	39

4. References	42
Appendix A: Customer Requirements	A-1
Appendix B: Verification Plan for the Conceptual Design	B-1
Appendix C: Test Plan for the Constructed Design Prototype	C-1
Appendix D: Final Design Specifications	D-1
Appendix E: Verification Data	E-1
Appendix F: Prototype Test / Measurement Data	F-1
Appendix G: FYDP Resources	G-1

List of Figures

Figure 1. Schematic of GeneDetek detection workflow.....	15
Figure 2. EC-LFAs with various electrode configuration integrated into LFA [1].....	16
Figure 3. GeneDetek Prototype	22
Figure 4. HPP and G>A transition for CYP2C19*2 mutation.	23
Figure 5. 3D Model of Prototype Encasing.	24
Figure 6. Bar graph showing specificity for CYP2C19*2 gene.	26
Figure 7. Working prototype calibration curve.	27
Figure 8. Residuals behavior analysis around zero.....	29
Figure 9. CV curve in PBS vs Artificial Saliva of blank and 5nM DNA concentration.	30
Figure 10. Bar graph representing the CV peak magnitude in PBS vs Artificial Saliva	30
Figure 11. Hybridization with 25nM target DNA for 1 hour.	31
Figure 12. Amperometry signal before and after incubating with HRP for signal amplification.	33

List of Tables

Table 1. Customer requirements summary.	10
Table 2. Specificity testing results.	25
Table 3. GeneDetek dimensions and comparison with threshold values.	31
Table 4. Side-by-side comparison of the Test Results versus the Customer Requirements.....	34

1. Introduction

1.1 Problem statement

Prescribing medications to individuals diagnosed with depression usually involves a trial-and-error process, where the patient is exposed to various antidepressants. However, over 60% of patients experience recurring depression symptoms following their first major depressive episode [1]. These relapses stem from significant pharmacogenetic differences among individuals, affecting drug metabolism and response.

Pharmacogenetic testing is a promising alternative to this trial-and-error approach since it helps to identify genetic mutations impacting medication responses and provides personalized medication recommendations. Regrettably, these tests face limited adoption in healthcare due to high costs and demanding laboratory resources.

Thus, our goal is to develop a non-invasive, affordable, and user-friendly electrochemical biosensor capable of detecting single nucleotide polymorphisms (SNPs) in the CYP2C19 gene that are associated with poor responses to commonly prescribed antidepressants. This biosensor uses saliva as the target analyte, a single-stranded DNA (ssDNA) sequence in a hairpin conformation as the biorecognition element, and electrochemistry as the transduction tool.

1.2 High-Level Description of The Design

Our design approach will rely on a commercial DNA extraction kit to process the saliva samples, a screen-printed electrode (SPE), a potentiostat to measure changes in electrochemical signal, and a data processing software to determine the results and generate a report. Specifically, in this approach the electrode's surface will be functionalized with MCH and a ssDNA sequence complementary to the CYP2C19*2 SNP. Such ssDNA sequence was designed to take a hairpin

conformation and is dually labelled with biotin and a thiol group, this will be referred to as hairpin probe. In the presence of the target SNP, the hairpin probe will open, hybridize, and take the typical duplex conformation of DNA exposing the biotin label on the hairpin probe. After that, the enzymatic probe horseradish peroxidase conjugated to streptavidin (HRP-streptavidin) is incubated and a solution with 3,3',5,5'-tetramethylbenzidine (TMB) and hydrogen peroxide H₂O₂ is introduced to the system. The presence of HRP in the TMB-H₂O₂ solution results in a change in current that can be quantified with the use of a potentiostat. The raw data file of the potentiostat is then uploaded to the GeneDetek App that uses the calibration curve of the sensor to return the results and print out a comprehensive report with the information of the patient, a list of recommended medications based on the presence or absence of the gene mutation, and the outlined detection method.

1.3 Customer Requirements

The proposed device will be designed to fulfill the requirements summarized in the table below. For more details on the customer requirements look at Appendix A.

Table 1. Customer requirements summary.

Description	Characteristics			
	Functional	Non functional	Minimum specification	Performance
Primary Requirements				
1. Specific to polymorphism CYP2C19*2	x		>95% concordance rate with standard establishing methods	

2. Sensitive to low concentrations	x		<10nM
3. Target to saliva sampling	x		Total error within 10% tolerance
4. Point-of-care design	x		5-20 cm width 15 - 20 cm length 10 - 20 g weight
Secondary Requirements			
1. Rapid Testing and Detection	x		Within 24 hours
2. Cross-Reactivity	x		None
3. Small Sample Volume Compatibility	x		A spit of saliva (~ 5 ml)
4. Usability and User Friendly		x	Instructions' Manual

1. Specific to polymorphisms CYP2C19*2 allele

The cytochrome P450 CYP2C19*2 was selected due to its association with several antidepressants of interest [2]. This allele is identified as coding for defective enzymes that are part of the drug metabolism process within the body. Considering that CYP2C19*2 allele decreases the metabolism of certain prescribed antidepressants, detecting this gene is a key goal of the electrochemical biosensor [3].

2. Sensitive to low concentrations

The limit of detection (LOD) must be low enough to detect minimum amounts of concentration of target analyte within saliva. Ideally, literature has verified that trace amounts of

the target analyte are present in saliva at concentrations as low as 50 ng in 2 mL of sample [4]. More information on this can be seen in Appendix A. Therefore, it is ideal to have an LOD that is low enough to compete with other biosensors currently published in literature. The minimum concentration for detection is outlined in the customer requirements table above.

3. Target to saliva sampling

Considering that the alternative is an invasive blood sample, providing customers with a non-invasive and simple method to collecting their genetic information is a solution that can be marketable. A non-invasive collection method that is simple and easy to use will increase the chances of patients undertaking this option, enabling better patient co-operation.

Saliva was chosen for its ease of acquiring. In comparison with other non-invasive mediums, saliva is almost always present and able to be collected at any time. More information can be found in Appendix A.

4. Point-of-care design

Point-of-care design is important for ease of use and minimizing the amount of space required in laboratory settings. Ideally, this device should be small enough to be easily shippable, easily moveable, and small enough to be used as a hand-held device. The compact design should ensure ease of use.

Secondary Requirements

1. Time for Test Completion and Result Delivery (Rapid Detection)

The biosensor must produce results within 24 hours of starting the test to ensure that rapid detection is met. This provides a competitive advantage over commercial solutions by ensuring that users can make informed decisions within a day of testing.

2. Non Cross-Reactive

Cross-reactivity should be addressed to ensure that the components of the biosensor are working as intended and that the biosensor itself can work in non-ideal conditions. Ideally, the biosensor's detection components must amplify the signal only when hybridization of the target analyte occurs. To ensure this, testing must be done on the amplification enzyme used in this biosensor workflow. Additionally, examining the biosensor's response to bacterial contamination normally found in the mouth is also key to ensuring that the biosensor will work in non-ideal conditions. More information can be found in Appendix A.

3. Small Sample Volume Compatibility

Considering there is a limited amount of saliva a patient can produce at a time, small sample compatibility is key to making a user-friendly biosensor. A sensor capable of detecting within 5-7 mL of sample volume is important for ease of use and acquiring accurate results.

4. Usability and User Interface

Intuitive and user-friendly instructions are key to providing a good commercial experience. The biosensor should come with a manual and be simple to use to prevent any human error from inhibiting the accuracy of the results. Additionally, results interpretation should be clear and easy to follow for any user who is not familiar with reading voltametric results.

2. Discussion

This biosensor will detect the CYP2C19*2 SNP by deriving DNA from saliva samples and utilizing electrochemistry measurements. On the surface of a gold screen printed electrode, a self-assembled monolayer (SAM) consisting of MCH and thiolated hairpin probes will be immobilized. This modification will provide two functions, namely: to passivate the surface and prevent non-specific binding and to offer specific conjugation sites for the targeted binding of the hairpin probes. The hairpin probe, which is dually labelled with biotin and a thiol group, targets the

CYP2C19*2 SNP by employing a sequence that is complementary to the wild type allele through its loop portion. When in the presence of the complementary sequence, the hairpin probe will straighten into a duplex, exposing the biotin label. This is followed by the incubation with enzymatic probe horseradish peroxidase conjugated to streptavidin (HRP-streptavidin) which is known to have high affinity for biotin. Finally, a solution of 3,3',5,5'-tetramethylbenzidine (TMB) and hydrogen peroxide H₂O₂ is introduced to the system to induce electron transfer between TMB and H₂O₂ catalyzed by the presence of HRP. Such electron transfer results in a measurable change in current that can be quantified with the use of a potentiostat, in our approach we use cyclic voltammetry measurements. The raw data file is then uploaded to the GeneDetek App that takes the peak current measurement and fits it against our sensor's previously determined calibration curve to determine if the gene mutation is present or not. The app will also generate a comprehensive report summarizing the information of the patient, the recommended medications based on the results, and a brief outline of the detection method. See **Figure 1** for a schematic of the approach described.

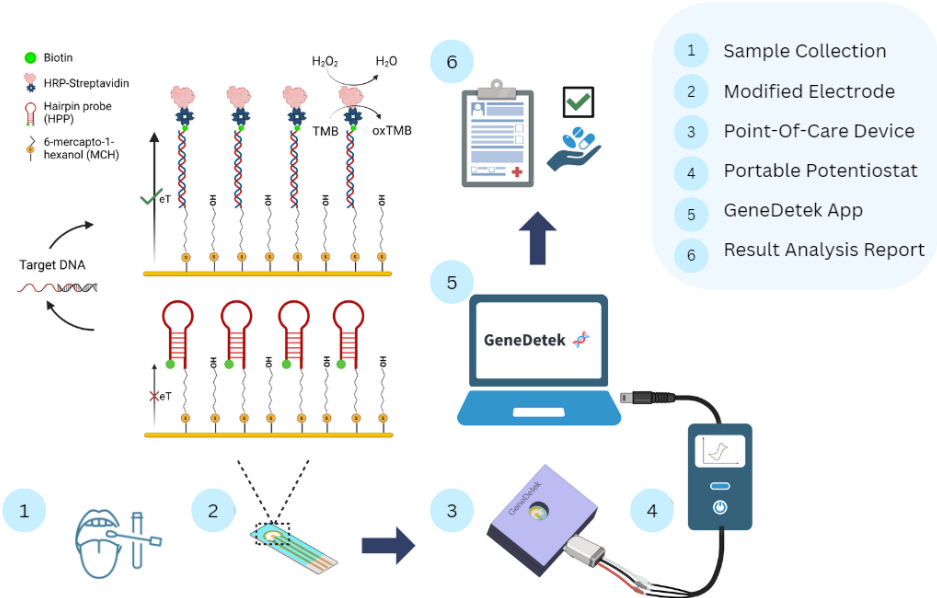


Figure 1. Schematic of GeneDetek detection workflow.

2.1 Design Choices

To address the need for an electrochemical biosensor that is affordable, user-friendly, and capable of detecting a SNP of the CYP2C19 gene, different approaches were considered based on literature review, materials, and time constraints.

The main alternative approach considered was an electrochemical lateral flow assay. The key aspects of that device included the design of biotin-labelled probes targeting the mutant CYP2C19 alleles for amplification refractory mutation system polymerase chain reaction (ARMS-PCR) which would have also incorporated an antigen in the target sequence. Then, the usage of single-walled carbon nanotubes (SWCNT) to maximize surface area for functionalization of an antibody that had affinity to the antigen in the biotin-labelled target amplicons obtained from ARMS-PCR. Resulting in the creation of a SWCNT-analyte complex at the conjugate pad if the target was present during ARMS-PCR. The electrochemical part of that device would have been

incorporated into the t-line and c-line where they would act as functionalized electrodes with a potentiostat attached with the ability to detect differences in voltage along the surface of the two lines. See Figure 2 for reference on the mechanism described.

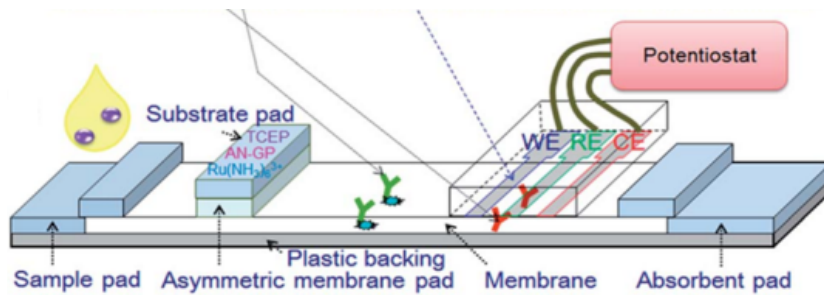


Figure 2. EC-LFAs with various electrode configuration integrated into LFA [5].

This approach was discontinued given that further literature review suggested limitations for sensitivity when using LFA, it required DNA amplification through ARMS-PCR, it relied on antibodies, and required different porous pad materials for its fabrication, all which amounted to a more complex and expensive detection system.

Thus, from a LFA strip our final designed transitioned to screen printed electrodes which offered improved biosensor performance, cost-effectiveness, surface stability and versatility. Specifically, the design included Phase Zero SPEs by CTI which have shown higher electroactive surface area compared to commercially available high-temperature curing ink or low-temperature curing ink electrodes [7]. Our search suggested that monolayers formed on gold SPE with uniform surface may be more stable compared to other electrodes, leading to more consistent and reproducible biosensor performance [7]. On top of this, the gold surface of the Phase Zero SPEs can be readily functionalized with thiolated DNA probes which are integral for our approach. From the design of probes to perform ARMS-PCR we transition to hairpin probes functionalized with biotin on one end and thiolated on the other end. Research suggested hairpin probes improve

specificity, enhance signal transduction, and are easy to functionalize and attach to electrode surfaces. Due to their unique stem-loop structure, hairpin probes allow for highly specific target recognition compared to linear ssDNA probes [9]. On top of this, it undergoes a conformational change upon target binding which can be transduced into a measurable electrochemical signal, allowing for sensitive and selective detection [9]. To aid sensitivity and address our customer requirement of targeting low concentrations of DNA, we implemented an enzymatic probe (HRP-streptavidin and TMB-H₂O₂) to further increase the electrochemical signal resulting from the conformational change of hairpin probes. With these changes and the use of a portable potentiostat our final approach allowed us to meet the customer requirements of point of care design, rapid testing, and small sample volume compatibility.

2.2 Design Verification

2.2.1 Design Verification Outline

The main aspects of the verification plan included the analysis of the theory behind the electrochemical transfer system in use. This included the examination of the redox system utilised and the cyclic voltammetry properties associated with such systems. Additionally, the capture mechanism and SAM system were also investigated in terms of characterization of the functionalized electrode surface. Cyclic voltammetry and impedance characteristics were utilised in an effort to verify the workings of the SAM. Finally, DNA folding simulations were used to determine the intended secondary structure required for the HPP. These structures were used to simulate the efficacy of the HPPs specificity to the intended target. More information is included in Appendix B.

2.2.2 Analysis of Verification Data

Electrochemical Electron Transfer System

The following section outlines the working theory behind the electrochemical transfer system of the biosensor detailed in this report. An electrochemical system is used to convert the hybridization of target DNA to the bioreceptor into an electrical signal, readable by a commercial potentiostat. This system utilises a redox molecule bound to one end of the hairpin probe through a biotin-streptavidin link, facilitating the exchange of charges on the electrode surface upon application of a potential voltage. During hybridization, two main changes occur on the electrode surface: (1) surface charge increases due to the presence of complementary DNA, (2) charge transfer resistance increases as the distance between the redox probe and electrode increases. As such, examining these phenomena is important for analysing the results of the electrical process.

It is observed in Appendix B that hybridization of an entirely complementary strand of DNA to the HPP will result in an efficient electron transfer flow that can result in a cyclic voltammogram of higher magnitude. However, hybridization with a mismatched strand will result in one of lower magnitude [9]. As such, this is an important phenomena tested to examine the specificity of the electrochemical biosensor. The results of this verification outline will be detailed in section 2.2.2.

The electrode surface was functionalized with a loosely arranged SAM to enable the likelihood of hybridization without steric hindrance. However, it is noted that for loosely arranged SAMs, the nature of the redox probes affect the electron transfer on the surface [10]. Consequently, the electrochemical system selected consists of HRP, hydrogen peroxide, and TMB. HRP helps facilitate the oxidation of TMB in the presence of hydrogen peroxide to generate the charge transfer system utilised for signal generation purposes. This can be quantified through the

Michaelis-Menten constant as detailed in Appendix B [11]. In the presence of varying potential voltage, the redox reaction behaves in a forward and reversible manner, amplifying the signal generated. The difference between the change in signal of the redox probe with respects to distance from the electrode surface and the change in signal due to redox reactions occurring on the surface of the electrode can be corroborated to the signal generated with and without HRP. Or it can be calculated through the use of the Michaelis-Menten equation and determination of a Lineweaver-Burk plot as detailed in Appendix B [11].

Capture Mechanism and Surface Coverage of Electrode

Functionalization of the electrode surface with a self-assembled monolayer (SAM) consisting of 6-mercaptophexanol and HPP is a key aspect of the biosensor's capture mechanism. The SAM was characterized through CV and impedance measurements taken after each step of the fabrication protocol. The expected behaviour is a reduction in CV signal as the layer is formed on the surface of the electrode while the curvature of the impedance measurement increases (corresponding to an increase in the charge transfer resistance) due to the biomolecules preventing diffusion. Further data for characterization theory and results can be seen in Appendix B and E, respectively.

Oligonucleotide Folding Simulations

DNA folding simulations were performed on the HPP prior to in-lab testing to validate that the intended secondary structures would occur naturally. The tools utilised to do this were OligoAnalyzer™ (tool licences UNAFold software) and UNAFold (formerly known as mFold). These tools were selected for their ability to predict secondary structures with high accuracy. A review analysing 9 different DNA folding softwares found that mFold could predict with an exact

accuracy of 46%. However, this accuracy increased up to 83% when including close predictions [1]. However, a limitation noted in all 9 softwares was the prediction of complex ssDNA structures with immobilising modifications. A solution-phase ssDNA structures may have different secondary structures compared with the same immobile ssDNA. Despite this, mFold can address this limitation by including suboptimal solutions which enables a 49% exact accurate prediction that increases up to 90% when including close predictions [12]. Consequently, mFold (and associated tools) was selected for its ability to predict with high accuracy and account for immobilising modifications on a sequence.

Initially, three HPP designs were selected for the evaluation to minimise the amount of unintended secondary structures. Further details on the three designs are detailed in Appendix E. The selected design consisted of the SNP closer to the 3' end with minimal unintended secondary structures within the loop portion of the probe. Folding simulations done on this sequence resulted in four main secondary structures. These simulations were used to compare the spontaneity of how likely the HPP would form its intended structure and the likelihood of unintended secondary structures occurring. A quick analysis table of the Gibbs free energy values given for the most stable secondary structures is also provided in Appendix E. To summarise, the most common structure to form was the intended secondary hairpin structure required for the HPP to operate. Following this, a second structure with an additional base pair in the stem region of the HPP was also likely to occur. However, this structure does not impede the function of the HPP. The last two structures had unwanted secondary structures in the loop portion of the HPP that could inhibit the function of the HPP. However, these structures were highly unlikely to occur due to their Gibbs free energy values. A Boltzmann's distribution was used to try and predict the percentage of each

secondary structure that may occur at room temperature and more details are provided in Appendix E. Overall, the intended secondary structure had the highest likelihood of occurring.

Simulations were also run to compare the spontaneity of how likely the test sequences would bind to the HPPs. A detailed table consisting of sequence length, GC content, melting temperature, molecular weight, and extinction coefficient for the hairpin probe and selected test sequences is detailed in Appendix B. In summary, the full hybridization of the target sequence resulted in a Gibbs free energy of -33.39 kCal/mol, hybridization of a sequence with one mismatch on the 3' end resulted in a Gibbs free energy of -31.44 kCal/mol, and hybridization of a sequence with two mismatches on the 3' end resulted in a Gibbs free energy of -27.19 kCal/mol. All three structures had secondary hairpin formations that could not occur naturally (i.e., positive Gibbs free energy, melting point below room temperature). More information on the exact secondary structures is provided in Appendix E.

2.2.3 Deviations from Verification Plan

The main deviation from the original verification plan involves the exclusion of the COMSOL simulations for the electrode surface materials. However, characterization was done through in-lab testing for by examining CV and impedance characteristics of the SAM after each deposition of the layer. More information on the characteristics of the SAM layer can be seen in Section 2.2.2.

PCR was removed from the final biosensor design so verification of the final amount of amplicons generated is no longer required. To determine the concentration of DNA used in the experiments, stock solutions of 100 μ M were made from the sequences acquired from external

vendors and split evenly into tubes that were stored in a freezer. These solutions were subsequently diluted when needed for experiments.

2.3 Prototype Construction

As mentioned in the introduction, the GeneDetek's solution involves an electrochemical biosensor designed to detect the CYP2C19*2 mutation, which is linked to poor responses to antidepressants. This biosensor offers a non-invasive, rapid, and cost-effective alternative to current pharmacogenetic testing methods. Illustrated in Figure 3 is the GeneDetek prototype alongside the components used in its assembly.

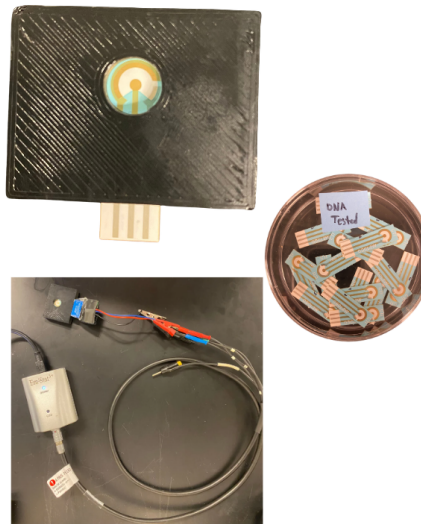


Figure 3. GeneDetek Prototype

The functional prototype of the GeneDetek biosensor was built using Gold Screen Printed Electrodes, specifically the “CTI Phase Zero SPE” model provided by PalmSens. Then, as shown in Figure 1, a Self-Assembled Monolayer (SAM) was formed on the working electrodes of the SPEs, creating the sensing interface for the detection mechanism of the GeneDetek biosensor. The SAM layer was created using 6-mercaptop-1-hexanol (MCH) and hairpin probes (HPP). The MCH

molecule is an important component of the SAM layer as the MCH's thiol groups bind strongly to the gold surface, preventing non-specific adsorption of proteins or contaminants, and providing space between the HPPs for optimal functionality. The HPP, procured from Sigma-Aldrich, was designed to have a complimentary sequence to the target DNA containing the genetic mutation for CYP2C19*2, as shown in Figure 4. And, attached to the HPP is a biotin label. When the target DNA of the genetic mutation hybridizes to a HPP, it causes a structural change in the HPPs, transforming their closed loop conformation into an open duplex and exposing the biotin label on one end of the HPPs.

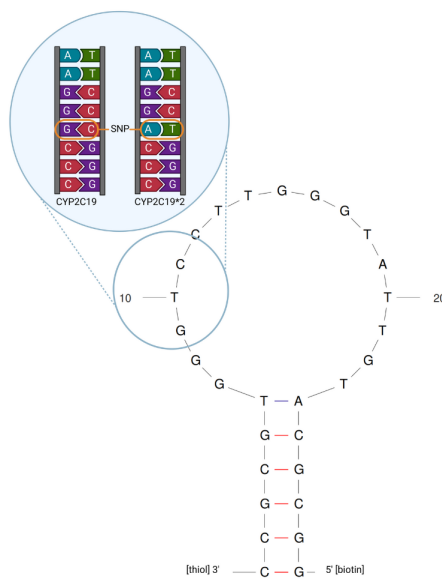


Figure 4. HPP and G>A transition for CYP2C19*2 mutation.

Biotin is a molecule that has high affinity to streptavidin, which is conjugated to the Horseradish Peroxidase (HRP) enzyme. When the target DNA is not present, the biotin is not accessible to the streptavidin-HRP complex due to the hairpin structure. Upon target binding and the consequent structural change, the biotin becomes exposed and can bind to the streptavidin-HRP. This complex can catalyze a reaction with TMB (tetramethylbenzidine) in the presence of hydrogen peroxide, resulting in an electrochemical signal that the GeneDetek sensor can detect.

Appendix D provides more description on how the HPP was designed as well as the fabrication steps to functionalize one SPE.

Signal transduction is accomplished using a potentiostat to measure the HRP-TMB redox reaction, with the results readily available through the GeneDetek software. The GeneDetek software is a user-friendly application developed with Streamlit. This application simplifies the user's interaction with the biosensor by providing a straightforward interpretation of the results. The code used to develop the app can be found in Appendix D.

Finally, in order to provide a Point-Of-Care design to the user and to protect the electronics of the biosensor, an encasing was designed using SolidWorks, with its 3D CAD representation displayed in Figure 5. The full specifications and design considerations for the encasing, as well as the materials used, are comprehensively detailed in Appendix D.



Figure 5. 3D Model of Prototype Encasing.

2.4 Test Results

The following test results are presented per customer requirement. The test results of the working prototype are included in the main report and test results of the different iterations to reach the final working prototype are included in Appendix F.

2.4.1 Primary Requirements

1) Specific to polymorphism CYP2C19*2

Selectivity was tested using 0 nM of target DNA, 20 nM of target DNA, mismatch-1, and mismatch-2. The respective results can be found in Table 2, including the current reading and the corresponding ratio. Two tests were taken using the same protocol and differential pulse voltammetry (DPV) found in Appendix F was used to display the comparison.

Table 2. Specificity testing results.

Test # / Ratio	Mismatch-1	Mismatch-2	Blank	Target DNA
Test 1 (uA)	7.895	132.5	1.36	25.2
DNA:Mismatch	3.1919:1	0.1902:1	18.5294:1	-
Test 2 (uA)	8.829	9.596	8.164	8.363
DNA:Mismatch	0.9472:1	0.8715:1	1.0244:1	-

It was observed that sequences including 1 mismatch resulted in slightly lower signals in comparison with the target sequence. Sequences involving 2 mismatches resulted in significantly higher signals on average. We achieved our expected 2:1 ratio of signal strength for target DNA to sequences with one mismatch but did not see the same result for ratios of target DNA to sequences with two mismatches. Additionally, we did achieve a signal ratio of target DNA to blank sample that was higher than the 3:1 ratio we had targeted in our test plan. Averaging the two results of the ratios for the test also resulted in a ratio that was greater than 3:1.

The following bar graph in Figure 6 can also visualize the differences between the mismatch-1 and target DNA current readings. This difference corroborates the specificity and ability of our biosensor to discriminate between mismatch-1 sequence and the target gene mutation.

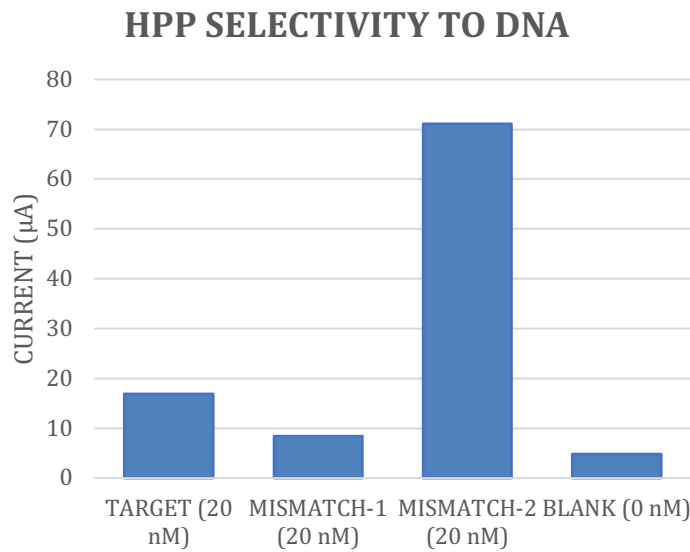


Figure 6. Bar graph showing specificity for CYP2C19*2 gene.

2) Sensitive to low concentrations

2.1) Signal-to-noise ratio (SNR)

The overall system has been developed using 1x PBS in nuclease free water as our main buffer. The SNR calculation consisted of comparing the magnitude of the peak signal at a known DNA concentration to the level of background noise present in the measurement system. The “Psignal” corresponds to the target DNA concentration of 15nM. The “Pnoise” was defined as the unwanted signal of the CV curve taken form the part of the voltammogram where no electrochemical reactions were expected to occur. Thus, Pnoise equals the standard deviation of this region.

$$SNR = \frac{P_{signal}}{P_{noise}}$$

$$SNR = \frac{3.327}{0.10}$$

$$SNR = 33.27$$

The resultant SNR value indicates that the signal stands out from the noise, which is important for reliable data interpretation in cyclic voltammetry measurements. Since the SNR is at least three times higher than the background noise (3:1) it is considered a pass.

2.2) Calibration Curve

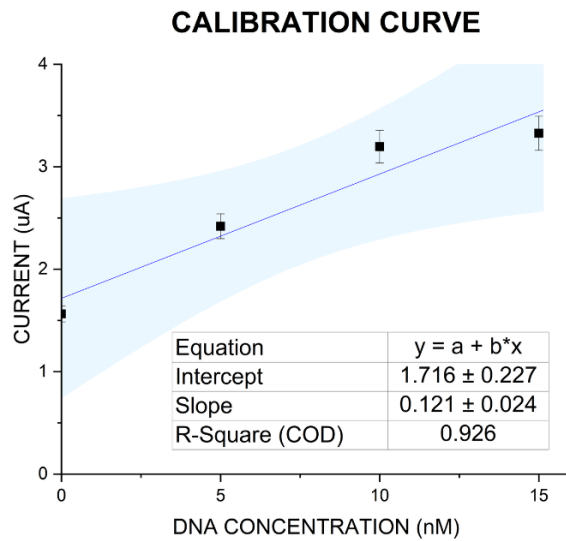


Figure 7. Working prototype calibration curve.

The final calibration curve shown in Figure 7 represents the quantitative relationship between the DNA concentration of the gene mutation in a sample (nM) and the corresponding electrical current measured in microamperes (μ A). The data used to make the calibration curve

was obtained from experiments performed on two different days replicating the same experimental conditions.

As evidenced by the curve, there is a linear increase in current with the concentration of the target DNA, suggesting the biosensor's response is directly proportional to the DNA concentration. A linear regression model was used to fit the data points. The linear equation used was $y = 0.121x + 1.716$, where the slope, indicating the change in current, is $0.121 \mu\text{A/nM}$. And the intercept is given by $1.716 \mu\text{A}$, which represents the response to a sample without the gene mutation. Moreover, the R value or coefficient of determination of 0.926 evidenced a strong positive linear relationship between the DNA concentration and the measured current.

2.3) Limit of Detection (LOD)

The LOD was calculated using the formula shown below, where the blank value used was the standard deviation of the blank sample's response and the slope values was taken from the calibration function equation.

$$LOD = 3.3 * \frac{\text{Blank}}{\text{Slope}}$$

$$LOD = 3.3 * \frac{0.153}{0.121}$$

$$LOD = 4.173 \text{ nM}$$

Solving this equation, it was found that the LOD of the GeneDetek biosensor was 4.17 nM . The resulting LOD was below the literature reference of 10nM limit of detection from saliva sampling, indicating that our sensor is capable of accurate detection of the target gene mutation in saliva samples.

2.4) Linearity

The linearity analysis of the calibration curve consisted of analyzing the residuals of the current measurements in the calibration curve and identifying if they behave randomly around zero. The analysis was done using the software Origin 2024. As it can be seen in Figure 8 the residuals do not have a specific pattern as two data points are above zero and two are below. Thus, corroborating the linearity nature of the calibration curve and considered a pass.

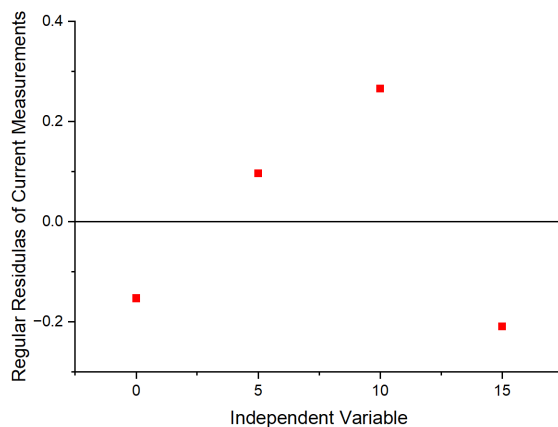


Figure 8. Residuals behavior analysis around zero.

3) Target to saliva sampling

The sensor was exposed to non-ideal conditions by the use of commercial artificial saliva. Artificial saliva was used as dilution buffer for the selected target DNA concentration. Thus, introducing contaminants to the system as opposed to using PBS. A shift of the peak in the CV curve towards positive potentials was observed suggesting that the addition of contaminants to the system affected the electrochemical behavior as seen in Figure 9. However, the magnitude of the peak was comparable to the trend observed under controlled conditions using PBS showing promising results towards our sensor performance in saliva samples as seen in Figure10.

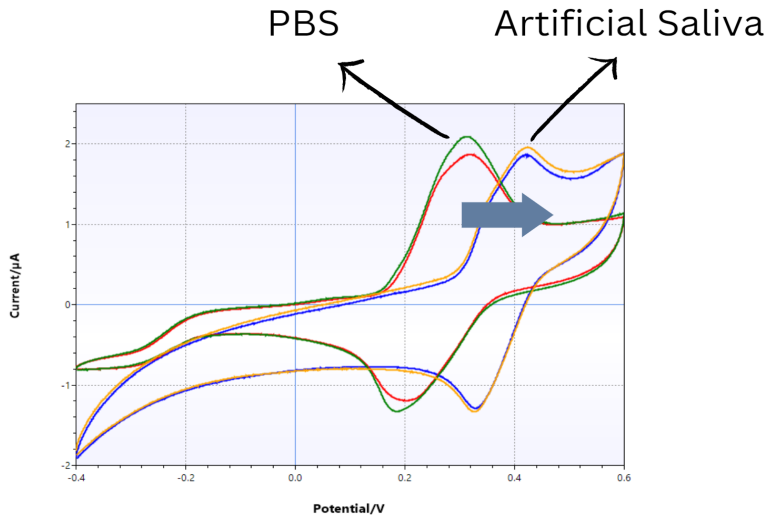


Figure 9. CV curve in PBS vs Artificial Saliva of blank and 5nM DNA concentration.

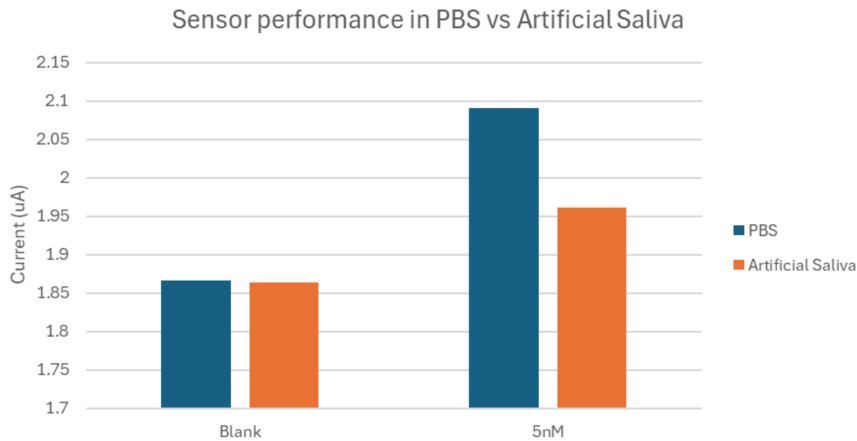


Figure 10. Bar graph representing the CV peak magnitude in PBS vs Artificial Saliva

4) Portability & Ergonomics

The portability and ergonomics analysis considered the screen-printed electrode (SPE) and 3D printed encasing. The potentiostat was not considered part of the final device design since it was out of our scope. Instead, a portable potentiostat from PalmSense (Emstat3) was used. The analysis was achieved by measuring and recording the weight and dimensions of the device. Table

x includes the final dimensions of the GeneDetek biosensor and compares the design's dimensions against the threshold values established in our customer requirements.

Table 33. GeneDetek dimensions and comparison with threshold values.

Dimensions	Threshold	Measured	Pass <input checked="" type="checkbox"/> / Failure <input type="checkbox"/>
Weight	< 20 g	10.68 g	<20 g Pass <input checked="" type="checkbox"/>
Length	< 20 cm	3.2 cm	<20 cm Pass <input checked="" type="checkbox"/>
Width	< 20 cm	4.0 cm	<20 cm Pass <input checked="" type="checkbox"/>

2.4.2 Secondary Requirements

1) Rapid Testing and Detection

1.1) Hybridization

Three different hybridization times were analyzed. The measurements were taken at 20, 45 and 60 minutes following the deposition of the target DNA onto the electrode using a concentration of 25 nM of target DNA. The hybridization time chosen for the working prototype was 1 hour as seen in Figure 11. The analysis of the different hybridization times can be found in Appendix F.

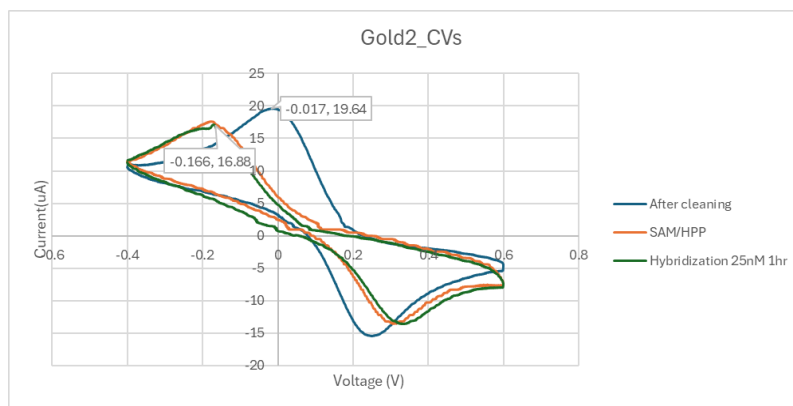


Figure 11. Hybridization with 25nM target DNA for 1 hour.

1.2) Reaction Time Assessment

To determine the overall reaction time, the time starting at the saliva collection until the output of results was considered. The estimated times outlined in the DNAGenotek protocol for sample preparation and DNA extraction were used. Then, for the biosensor signal reading and result analysis, the experimental values observed during the experiments in the lab were included.

The reaction time assessment resulted as follows:

- Collection of the saliva sample: ~5 min
- Saliva sample preparation and DNA extraction and purification: ~ 5 hours and 10 min
- Biosensor signal reading: ~1 hour and 40 min
- Analysis of Results: ~ 5 min

The estimated total reaction time is ~ **7 hours**. The reaction time resulted <24 hours thus it was considered a pass.

2) Cross-Reactivity

2.1) HRP influence in signal

To evaluate the cross-reactivity of the signal amplification method, amperometry measurements were taken before and after adding HRP to the hybridization of 25nM of target DNA to the system. It can be seen in Figure 12 that there was a significant amplification in signal with a ~30-fold increase.

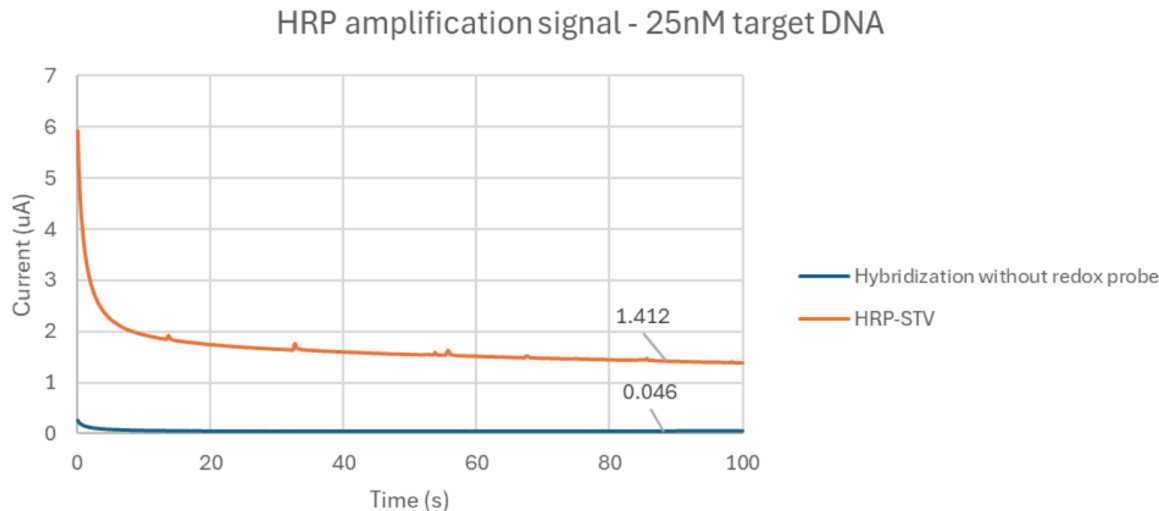


Figure 12. Amperometry signal before and after incubating with HRP for signal amplification.

2.2) Bacterial Contaminants

Bacterial contaminants found in the oral cavity was also considered as a method for testing cross-reactivity. Ideally, further testing with a saliva-based environment containing natural bacterial DNA was proposed to test how well the device could operate in non-ideal conditions. While additional contaminants were not tested, section 3 detailing the Targeting to saliva sampling indicates the sensor's ability to operate under non-ideal conditions with the contaminants present in the artificial saliva. Additionally, due to limitations in budget and limited number of electrodes, testing of target and non-cognate sequences with and without contamination was not performed. In the future, further testing should be done to understand the full extent of effects that bacterial contamination has on the biosensor.

3) Small Sample Volume Compatibility

Tests performed in ideal conditions (target DNA in PBS) required ~30uL of solution to hybridize to the hairpin probes and generate a change in electrochemical signal, such volume is

enough to cover the circular area of the working electrode of the SPE. Similarly, tests performed with target DNA in artificial saliva required that volume. As for testing with real saliva, the estimated volume needed to be processed with the Oragene DNA extraction kit is 10mL. Those 10mL are further processed to get rid of contaminants and extract ssDNA. Comparably, a small sample volume from the yield of the extraction kit would be needed to incubate on the electrode surface, which is ~30uL. This proves that our detection mechanism is compatible with saliva sample volumes as small as 10mL, and even smaller quantities when considering an already purified sample, where the volume needed goes down to 30uL which is enough to cover the working electrode of the SPE.

4) Usability and User Friendly

The Point-of-Care Design verification's usability test aimed to assess how user-friendly the GeneDetek sensor was. Due to time constraints, we were not able to ask feedback from the users, in this case students. However, the development of an app for the interpretation of the results helped in simplifying the steps of the workflow, making it easier for the user to analyze the results obtained from the biosensor.

Overall, the presented results from the comprehensive test plan conclusively demonstrate that the customer requirements were met as seen in Table 4.

Table 4. Side-by-side comparison of the Test Results versus the Customer Requirements.

Primary requirements	Test quantifiers	Pass/fail criteria	Pass/Fail Results
1) Specific to polymorphism CYP2C19*2	Compare signal ratios of target DNA to mismatch DNA	3:1 target sequence to non-cognate sequence	Target:Blank = 9.776:1 ✓
		2:1 target sequence to 1- and 2-mismatch	Target:M1 = 2.069 :1 ✓ Target:M2 = 0.5308 :1 ✗
2) Sensitive to low concentrations	Calibration curve/linearity	Linear calibration curve	Linear ✓
	SNR	SNR is at least three times higher than the background noise	SNR = 33.27 ✓ Noise = 0.10 uA ✓
	LOD	Value <10nM or >3SD	LOD = 4.173 nM ✓
3) Target to saliva sampling	Compare the signal response of target DNA in artificial saliva to the signal response of target DNA in Phosphate buffer saline	Total error within tolerance of 10%	Ongoing
4) Test for Portability and Ergonomics	Compare the design's dimensions against the threshold values	<20 g, <20 cm, <20 cm	The final dimensions of the GeneDetek biosensor are: Weight = 10.68g ✓ Length = 3.2 cm ✓ Width = 4.0 cm ✓ Height = 8 mm (not considered in the requirements)
Secondary requirements			
1) Rapid Testing and Detection	Hybridization time	Perform fluorescence measurements at different time intervals, time should be < 24h.	Instead of fluorescence measurements, CV and Impedance measurements were performed at different times to determine hybridization.

			Hybridization time: 1 hr <input checked="" type="checkbox"/>
	Reaction Time Assessment	Time to: 1) collect a saliva sample, 2) prepare the saliva sample, 3) place the specimen on the biosensor and obtain a signal, and 4) analyze the results; is <24hr	Total time: ~ 7 hours <input checked="" type="checkbox"/>
2) Cross-Reactivity (with/without HRP)	Conduct test of signal ratios with target sequence and non-cognate sequences with and without contamination	Signal ratios of 2:1 between the target sequence and non-cognate sequences	ongoing
3) Small Sample Volume Compatibility	Consistent with the LOD Test results	Concentration below 10nM	LOD = 4.17 nM <input checked="" type="checkbox"/>
4) Usability and User-Friendly	Usability test	The user interface must be easy to follow.	User friendly <input checked="" type="checkbox"/>

2.5 Deviations/Shortfalls

In this section, we examine any deviations from the initially defined design of the GeneDetek biosensor and the shortfalls in meeting our primary customer requirements outlined in Appendix A.

2.5.1 Opting Out of Gold Nanoparticles (AuNPs) on Carbon Electrodes

During the design phase of the GeneDetek biosensor, a decision to stop the functionalization of AuNPs on carbon electrodes was made. The main reason to use AuNPs was to enhance the sensitivity of the biosensor. However, it was observed that over time, the nanoparticles were not stable as they exhibited a tendency to aggregate, increasing their particle

size and polydispersity. The SEM images showing aggregation of the AuNPs and the DLS measurements can be found in Appendix E.

The aggregation of AuNPs can significantly alter the electrochemical properties of the sensing interface as well as the sensitivity of the sensor. Having aggregation over time can lead to inconsistent and unreliable measurements, as well as less long-term stability. Consequently, we chose to use screen printed gold electrodes instead, which are more conductive than carbon electrodes and more stable than AuNPs.

2.5.2 Changes in protocol for MCH

The initial protocol for the deposition of a SAM made of MCH and hairpin probes seemed not to aid in the linearity of our sensor, where an increase in target DNA concentration was expected to translate to a higher current peak. A paper by T. Kjallman, et al. suggested that the issue was related to high surface coverage and steric forces halting the hybridization of the hairpin probes and the target [8]. To reduce the saturation on the surface of the electrode the concentrations of both hairpin probes and MCH were reconsidered. Given that the hairpin probe is essential for the binding and recognition of the target, its concentration for the immobilization step was kept constant at 1uM, but the incubation time was reduced from 1.5h to 1h. MCH concentration was dropped from 10 mM to 50uM corresponding to a ration of 1:50 with the hairpin probe. This was concluded based on the deposition protocol used by [8]. However, its incubation time was increased from 20mins to 1h.

The experiment with the second protocol for a SAM of 1uM hairpin probe and 50uM MCH showed even more variable results among different concentrations of target DNA. Therefore, the final SAM consisted of 1uM hairpin probe and 10mM MCH as explored in the results section.

2.5.3 Failure of Mismatch 2

Mismatch-2 failed to produce results that could fulfill customer requirements for specificity to mismatch-2. In short, while testing for HPP specificity, a targets sequence that was complementary to the HPP, a sequence with one mismatch to the HPP, and a sequence with two mismatches were examined and compared. Additionally, blanks were measured to set a baseline. It was observed that the average of the two tests resulted in the blank having the lowest DPV amplitude, the mismatch-1 having the second lowest, the target sequence having the second highest, and the mismatch-2 sequence having the highest DPV values.

It can be said that solution-phase DNA probes have high discriminatory abilities against SNPs while immobilized probes have less ability to discriminate as demonstrated in literature [13][14]. This would make sense if mismatch-1 and mismatch-2 were both higher or similar to the target strand. However, since only mismatch-2 is higher, it is hard to argue that this is the only reason why the results of the specificity tests have a strange trend. Additionally, these results conflict with the DNA folding simulations performed on the test sequences. The results of these simulations suggest that mismatch-2 should have the least amount of hybridization.

Another reason may have been that the results for mismatch-2 in the first specificity tests was an outlier. The signal generated from mismatch-2 in the test was more than 5x the signal generated for the target sequence and more than 10x the signal generated by mismatch-2 in the second set of specificity tests. However, more tests would need to be conducted to rule out this measurement as an outlier.

For future steps, validation of hybridization occurring is key to understanding and rationalizing the results of specificity for the HPP. Ideally, a validation test to be performed before electrode testing would be surface plasmon resonance of DNA hybridization on the sensor surface.

In the event that hybridization occurs, this should result in a change of refractive index which can be detected and attributed to the characterization of hybridization.

3. Summary

To conclude, this report details the entire engineering analysis and design considerations used in the making of an electrochemical biosensor for the detection of SNPs. Throughout this eight-month period, the biosensor has undergone several major design iterations in an effort to achieve a prototype that fulfils the customer requirements detailed in earlier sections. Mainly, this biosensor addresses the issues surrounding pharmacogenetics and the problems arising from poor uptake of prescribed drugs due to genetic influences. A point-of-care, fast, non-invasive, and cost-effective biosensor for the detection of genetic mutations is key to enabling informed decisions for the prescription of drugs.

The main objectives for this biosensor to fulfil included: (1) specificity to polymorphism CYP2C19*2, (2) sensitivity to low concentrations of the target sequence (i.e., an LOD < 10 nM), (3) ability to in saliva, (4) point-of-care design. The secondary requirements included: (1) rapid testing and detection in under 24 hours, (2) minimization of cross-reactivity, (3) small sample volume compatibility (~ 5 mL of saliva), (4) user-friendly for end users. All four main objectives were examined through in-lab tests to verify if the device could fulfil the requirements. The secondary requirements were fulfilled through a mixture of in-lab tests and the addition of a python application to analyse and generate a report of the results.

Consequently, the main design approach involved an electrochemical biosensor utilising a HPP bioreceptor. The electrochemical portion of the biosensor was selected due to the sensitivity it could yield when signal amplification occurred while the HPP portion of the biosensor was

selected due to its ability to discriminate genetic mutations. Ideally, the biosensor was split into four sections: (1) functionalization of the electrode, (2) capture mechanism, (3) electrochemical detection mechanism, (4) generation of results. The functionalization of the electrode included the formation of the SAM on the gold electrode surface. This was accomplished through the use of thiol-alkanes such as 6-mercaptophexanol and a thiol-modified HPP. Through a spontaneous thiol-gold linkage, the electrode surface was functionalized with HPPs and a SAM. This provided the necessary HPPs on the electrode surface for target sequence detection and also provided passivating effects against non-specific binding. The capture mechanism involved the hybridization of a target strand to HPPs. This enabled a change in conformation from a closed-loop conformation to a linear duplex, exposing the biotin-modified end of the HPP. The electrochemical detection mechanism was able to use this exposed biotin to conjugate HRP-streptavidin to the electrode surface, enabling the preparation for redox reactions. The oxidation of TMB from hydrogen peroxide in the presence of HRP enabled signal generation that was produced by a commercial potentiostat. Finally, results were cross-references automatically through the GeneDetek application and a report was generated using the software developed. Overall, the design approach focused on the generation of a signal on the electrode surface when target analyte was present.

The results of in-lab testing displayed that the device had a LOD under 10 nM and was able to function comparably under non-ideal environments (i.e., in saliva). Additionally, the final electrode encasing was able to fit within the POC design parameters. However, specificity to SNP CYP2C19*2 displayed conflicting results as detailed in the section labelled Deviations/Shortfalls. The device was able to meet all secondary requirements as testing results were generated within a 7 hour period, the device was able to work in non-ideal environments, the sample volumes

collected were less than 5 mL, and the user-friendly design came in the form of a python application and associated user-manual. In summary, all primary and secondary customer requirements except for specificity of probe to mismatch-2 were fulfilled.

Future work to be undertaken includes further testing and validation of the specificity of the HPPs. Beyond simply using folding simulations, testing undertaken to verify hybridization is occurring normally and that the modifications on the HPP are not inhibiting its' function are needed. Moreover, this can include the utilisation of the HPPs in solution phase (i.e., free-floating in solution rather than immobilised) with the use of fluorescence and quenching to examine their ability to discriminate target sequences while not immobilised. As it has been mentioned in literature, solution-phase HPPs have high ability to discriminate SNPs whereas the discriminatory ability of immobilised HPPs are significantly less effective [S3][S4].

Furthermore, multiplexing and the testing of a modular probe is also a key requirement for the establishment of a product platform. Ideally, the end goal of GeneDetek is to create a detection platform that can enable the detection of multiple SNPs to provide healthcare providers with the information they require to make informed decisions. The ability to multiplex and have multiple working probes is key to providing an array of data that can provide full context of the patient's potential reactions to certain prescribed drugs.

In summary, this report encapsulates the engineering analysis and considerations involved in developing an electrochemical biosensor for SNP discrimination and the tools used to interpret the results. This biosensor aimed to address critical issues in pharmacogenetics to ensure the informed prescription of drugs based on genetic influences.

4. References

- [1] A. I. Campos et al., “Understanding genetic risk factors for common side effects of antidepressant medications,” *Communications Medicine*, vol. 1, no. 1. Springer Science and Business Media LLC, Nov. 09, 2021. doi: 10.1038/s43856-021-00046-8.
- [2] Y. Xuhong et al., “A PCR-lateral flow assay system based on gold magnetic nanoparticles for CYP2C19 genotyping and its clinical applications,” *Artificial Cells, Nanomedicine, and Biotechnology*, vol. 47, no. 1. Informa UK Limited, pp. 636–643, Mar. 15, 2019. doi: 10.1080/21691401.2019.1575841.
- [3] M. M. Jukić, T. Haslemo, E. Molden, and M. Ingelman-Sundberg, “Impact of CYP2C19 Genotype on Escitalopram Exposure and Therapeutic Failure: A Retrospective Study Based on 2,087 Patients,” *American Journal of Psychiatry*, vol. 175, no. 5. American Psychiatric Association Publishing, pp. 463–470, May 2018. doi: 10.1176/appi.ajp.2017.17050550.
- [4] J. J. Swen et al., “Feasibility of pharmacy-initiated pharmacogenetic screening for CYP2D6 and CYP2C19,” *European Journal of Clinical Pharmacology*, vol. 68, no. 4. Springer Science and Business Media LLC, pp. 363–370, Oct. 08, 2011. doi: 10.1007/s00228-011-1130-4.
- [5] Perju, A., Wongkaew, N. Integrating high-performing electrochemical transducers in lateral flow assay. *Anal Bioanal Chem* **413**, 5535–5549 (2021). <https://doi.org/10.1007/s00216-021-03301-y>
- [6] Zamani, M. et al. (2022) Surface requirements for optimal biosensing with Disposable Gold Electrodes, ACS measurement science au. doi: 10.1021/acsmeasurescian.1c00042

- [7] Huang, J., Wu, J. and Li, Z. (2015) Biosensing using hairpin DNA probes, De Gruyter. doi: <https://doi.org/10.1515/revac-2015-0010>
- [8] Kjällman, T.H. et al. (2008) ‘Effect of probe density and hybridization temperature on the response of an electrochemical hairpin-DNA sensor’, Analytical Chemistry, 80(24), pp. 9460–9466. doi:10.1021/ac801567d.
- [9] A. R. Arnold, M. A. Grodick, and J. K. Barton, “DNA Charge Transport: from Chemical Principles to the Cell,” Cell Chemical Biology, vol. 23, no. 1. Elsevier BV, pp. 183–197, Jan. 2016. doi: 10.1016/j.chembiol.2015.11.010.
- [10] A. Abi and E. E. Ferapontova, “Unmediated by DNA Electron Transfer in Redox-Labeled DNA Duplexes End-Tethered to Gold Electrodes,” Journal of the American Chemical Society, vol. 134, no. 35. American Chemical Society (ACS), pp. 14499–14507, Aug. 23, 2012. doi: 10.1021/ja304864w.
- [11] M. Li et al., “Multiple effects of sodium dodecyl sulfate on chromogenic catalysis of tetramethylbenzidine with horseradish peroxidase,” Journal of Dispersion Science and Technology, vol. 42, no. 4. Informa UK Limited, pp. 526–536, Dec. 19, 2019. doi: 10.1080/01932691.2019.1702050.
- [12] T. Binet et al., “Comparative Study of Single-stranded Oligonucleotides Secondary Structure Prediction Tools,” BMC Bioinformatics, vol. 24, no. 422, 2023. doi: 10.1186/s12859-023-05532-5.
- [13] Y. J. Zheng et al., “Enzyme-based E-RNA sensor array with a hairpin probe: Specific detection of gene mutation,” Sensors and Actuators B: Chemical, vol. 181, pp. 227-233, May. 2013. doi: 10.1016/j.snb.2013.01.051.

[14] S. Tyagi and F. R. Kramer, “Molecular Beacons: Probes that Fluoresce upon Hybridization,” Nature Biotechnology, vol. 14, pp. 303-308, Mar. 1996.

Appendix A: Customer Requirements

A.1 Customer Requirements

A.1.1 Primary Requirements

A.1.1.1 Specific to polymorphisms CYP2C19*2 and CYP2C19*17 alleles

The enzyme associated with activating several medications in the body is cytochrome P450 (CYP) 2C19 [A.1]. One of the target medications for our customer is escitalopram (Lexapro) which is a frequently prescribed antidepressant. The common variations known to affect the metabolism rate and response to the target antidepressant are CYP2C19*2 and CYP2C19*17 alleles [A.2]. The CYP2C19*2 allele has been identified as a loss-of-function mutation while the CYP2C19*17 allele has been identified as a gain-of-function mutation [A.2]. Thus, detecting these polymorphisms in the CYP2C19 gene is essential to the functionality of the electrochemical biosensor.

The concordance rate will be used to quantify the minimum performance for this requirement. The concordance rate helps quantify the similarity between two sets of data that share an attribute in common. The comparison will be done between our experimental data and the data obtained from an established sequencing method. The concordance rate should be greater than 95% to deem the electrochemical biosensor successful.

A.1.1.2 Sensitive to low concentrations

The electrochemical biosensor should be sensitive to low concentrations of the CYP2C19 gene found in the analyte. The sensitivity can be quantified by calculating the limit of detection (LOD) of the system. The LOD determines the minimum concentration that the electrochemical biosensor can reliably detect. In a study that detects the CYP2C19 gene polymorphisms in saliva,

the recorded LOD was 50ng in 2ml of sample collected using the Oragene DNA self-collection kit [A.3]. Thus, the electrochemical biosensor should be able to detect the target polymorphisms with DNA concentration as low as 25ng/ml.

A.1.1.3. Target to saliva sampling

It is relevant for our customers that the collection method of the sample is non-invasive and simple to collect. Having a non-invasive collection method will facilitate the patient's involvement in the treatment process. Collection methods for analytes like blood can be invasive for patients who fear needles or are too delicate to have blood drawn, thus posing an extra barrier to the procedure. Additionally, blood samples usually require pretreatments that can be time-consuming and expensive. Collection methods for analytes like sweat can involve the need to perform physical exercises or the need to wear uncomfortable artifacts for long periods of time. Therefore, we have identified that the best analyte that is both non-invasive and simple to collect is saliva. Additionally, there are commercially available self-collection saliva kits that already present an easy medium of collection for biosensing applications.

The minimum performance will be evaluated using the agreement rate. The agreement rate calculates how close are the results of two diagnostic methods. The agreement rate between our platform and a blood-based system should be greater than 85%.

A.1.1.4. Point-of-care design

Our target customers are mental health professionals capable of prescribing antidepressants. Thus, they will require a compact system that can be used within their office space. Point-of-care testing is defined as a diagnosis tool that can be operated outside a laboratory setup

and close to the patient being treated [A.4]. Consequently, we require a point-of-care design that would facilitate the treatment decision process.

The minimum performance will be a portable device that will have a range size of 5-20cm width and 10-30cm length.

A.1.2. Secondary Requirements

A.1.2.1. Time for Test Completion and Result Delivery (Rapid Detection)

The electrochemical biosensor must complete the test and provide the result within 24 hours of initiating the test request. This time frame encompasses the entire testing process from collecting the sample and executing the test (sample application and reaction) to the interpretation and notification of the final result to the user.

Time frame phases within the 24 hours:

- Collection of the sample
- Preparation of the sample
- Execution of the test involving sample application and reaction
- Interpretation of Results
- Result notification

A.1.2.2. Non-Cross-Reactive

Cross-reactivity is crucial to ensure the test results are accurate and reliable. The electrochemical biosensor detection components must not bind to substances other than the target

analyte for which the test is designed. Binding to the wrong component might lead to false positive results, causing the device to incorrectly indicate the presence of the analyte when it is not present.

To test for cross-reactivity, the sensor will undergo rigorous testing to validate the potential of cross-reactivity. One way to test cross-reactivity would involve exposing the test to components that are chemically alike to the target analyte, meaning that they have similar molecular structures. It is important to test the device's response to identify if the presence of these molecules might lead to a false positive result.

A.1.2.3. Small Sample Volume Compatibility

The electrochemical biosensor must be built to efficiently and accurately perform the required analysis and testing with a minimal sample amount. The electrochemical biosensor must be capable of using a sample volume of approximately 5-7 ml, approximately, which is equivalent to a spoon of saliva. This sample volume should be enough to produce accurate and reliable results.

A.1.2.4. Usability and User Interface

The electrochemical biosensor should have clear and intuitive instructions for use. A set of instructions including information on sample collection, sample preparation, sample application, interpretation of the results, and disposal should be attached to the device. In addition, the results should be easy to read and interpret for positive and negative results. Finally, the instruction manual should include information on the allowable time for obtaining the test results.

A.2 References

- [A.1] Y. Xuhong et al., “A PCR-lateral flow assay system based on gold magnetic nanoparticles for CYP2C19 genotyping and its clinical applications,” *Artificial Cells, Nanomedicine, and Biotechnology*, vol. 47, no. 1. Informa UK Limited, pp. 636–643, Mar. 15, 2019. doi: 10.1080/21691401.2019.1575841.
- [A.2] M. M. Jukić, T. Haslemo, E. Molden, and M. Ingelman-Sundberg, “Impact of CYP2C19 Genotype on Escitalopram Exposure and Therapeutic Failure: A Retrospective Study Based on 2,087 Patients,” *American Journal of Psychiatry*, vol. 175, no. 5. American Psychiatric Association Publishing, pp. 463–470, May 2018. doi: 10.1176/appi.ajp.2017.17050550.
- [A.3] J. J. Swen et al., “Feasibility of pharmacy-initiated pharmacogenetic screening for CYP2D6 and CYP2C19,” *European Journal of Clinical Pharmacology*, vol. 68, no. 4. Springer Science and Business Media LLC, pp. 363–370, Oct. 08, 2011. doi: 10.1007/s00228-011-1130-4.
- [A.4] CMLTO, “Point-of-care testing in Ontario,” College of Medical Laboratory Technologists of Ontario, http://www.cmlto.com/index.php?option=com_content&view=article&id=1369&Itemid=567 (accessed Sep. 17, 2023).

Appendix B: Verification Plan for the Conceptual Design

B.1 Theory of HPP Simulations

DNA Folding Simulations

Folding simulations will be performed on the HPP design selected to verify that the intended secondary structure will occur at room temperature. Additionally, these simulations will also be conducted to check if any unintended secondary structures may occur and the likelihood of them happening. The acquired data from this includes sequence length, GC content, melting temperature, and molecular weight. Additionally, thermodynamic analysis will be performed on the structures to verify the probability of hybridization amongst the various test structures. The tools in question used to verify these results will be IDT's OligoAnalyzer™ tool and UNAFold (i.e., mFold). Additionally, NCBI blast will also be used to correlate the HPP and test sequence to the intended genetic mutation within CYP2C19. An analysis of the data acquired can be found in Appendix E.

B.2 Electrochemical Electron Transfer System

DNA-mediated charge transfer

An electrochemical electron transfer system is used to translate the DNA hybridization event in the presence of the target mutation to an electrical signal to be read by the commercial potentiostat. This system consists of a redox probe attached to one end of the hairpin probe that will exchange charges with the electrode surface when a potential is applied. The charge transfer is mediated by the DNA π-stach and the alkane-thiol structure. When the DNA hairpin probe opens to undergo hybridization, two important charge changes happen: 1) the total surface charge increases due to the presence of the complementary DNA (cDNA) strand at the electrode surface

and 2) the overall charge transfer resistance (R_{ct}) or electron transfer (ET) efficiency from the redox probe to the electrode surface increases as the redox probe distance to the electrode increases [B.1]. Therefore, the main events that directly affect the magnitude of the resultant electrical signal will be analyzed as part of the design verification including charge transport efficiency through the DNA π -starch, and ET process of the redox probes.

It can be generalized that the charge transfer will happen vertically as the resultant dsDNA is expected to orient upwards as opposed to sideways due to the increase in total surface charge when hybridization takes place [B.2]. To understand the DNA-mediated charge transfer, two scenarios should be considered: charge transfer through a well-matched double-stranded DNA (dsDNA) and a mismatched dsDNA as seen in Figure B.1.

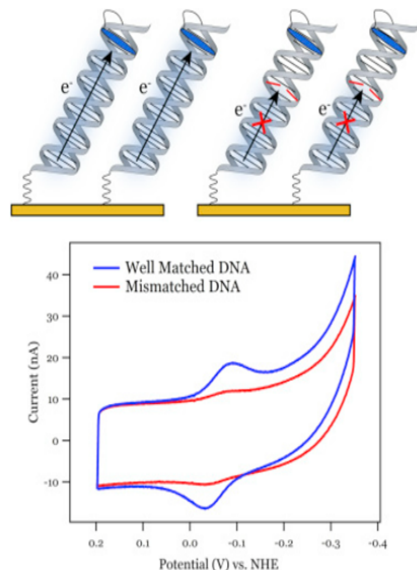


Figure B1. DNA-mediated charge transfer comparison depending on DNA structure [B.2]

The cyclic voltammogram in Figure A1 shows that electron transfer flow is efficient for the well-matched structure and discontinuous in the mismatch structure. Thus, resulting in a weakened current signal for the discontinuous case [B.2].

Our design takes advantage of the DNA-mediated charge transfer behavior to achieve one of our customer requirements that refers to specificity to polymorphisms CYP2C19*2. The hairpin probe contains the specific DNA sequence corresponding to the target mutation. When the cDNA hybridizes with the hairpin probe, the resulting DNA sequence will be well-matched. On the other hand, if non-specific DNA strands try to hybridize with the hairpin probe, the signal will be attenuated and distinguishable from the well-matched case.

Another factor to consider is the ET dependence on DNA probe density. Research suggests that the direct ET was evidenced in compact monolayers of tethered dsDNA to the electrode that contained a redox probe at the end of the helix structure [B.3]. However, when the monolayers are loosely arranged, the ET depends on the electrochemical nature of the chosen probes [B.3]. Our design uses a loosely arranged system as it increases hybridization likelihood and reduces steric hindrance between DNA strands. Therefore, the next section will focus on understanding the electrochemical characteristics of the chosen probes.

Redox probes

The electrochemical system consists of three main components: HRP, H₂O₂ and TMB. HRP is an enzyme that facilitates the transformation of chromogenic substrates. H₂O₂ is a colorless chemical compound that carries no charge. TMB is a chromogenic substrate that is used as a hydrogen donor in enzymatic assays. In the presence of HRP, TMB undergoes oxidation by H₂O₂, resulting in the production of a blue TMB diimine product and water byproduct as can be seen in Figure B.2. Blue TMB diamine **product**.

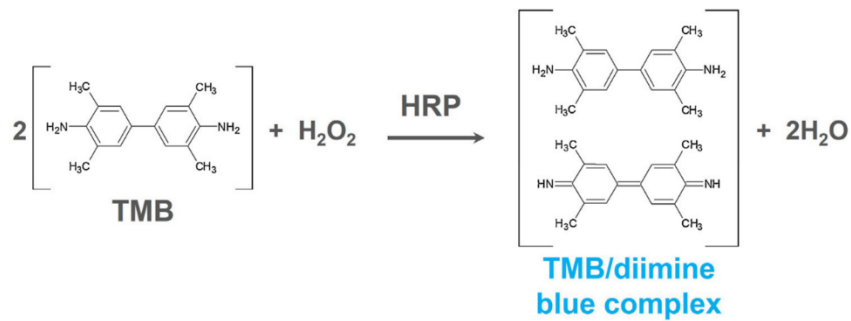


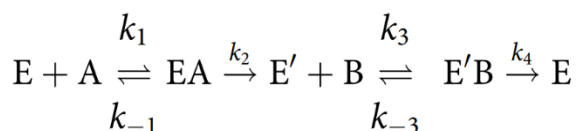
Figure B.2. Blue TMB diamine product [B.4]

This HRP - H_2O_2 - TMB system follows the enzyme kinetics. Thus, the Michaelis-Menten equation can be used to obtain the apparent kinetic parameters as follows [B.5]:

$$v_o = \frac{v_{max}[S]}{K_m + [S]}$$

Where v_o is the initial rate of product formation, v_{max} is the maximum rate assuming the infinite presence of HRP, $[S]$ is the substrate concentration and K_m is the Michaelis-Menten constant [B.5]. K_m will be based on literature standards and simulated.

Electrochemical reactions that use peroxidase for catalysis behave as a ping-pong mechanism. This mechanism leads to the following sequential reaction [B.5]:



Where E corresponds to HRP, A to H_2O_2 and B to TMB. Assuming steady-state and mass conservation, the initial rate of reaction would result in the following [B.5]:

$$v_o = \frac{v_{max} [H_2O_2][TMB]}{K_m^{H_2O_2}[TMB] + K_m^{TMB}[H_2O_2] + [H_2O_2][TMB]}$$

Where $K_m^{H_2O_2}$ and K_m^{TMB} refer to the Michaelis constant at saturated concentrations of TMB and H_2O_2 respectively. The resultant K_m values would correspond to each substrate value (TMB and H_2O_2) at which the concentration of the secondary substrate will remain constant and below its saturation concentration while changing the concentration of the primary substrate in the K_m value calculation, as seen in the following equations [B.5]:

$$K_m^{H_2O_2} = \frac{K_m^{H_2O_2}[TMB]}{K_m^{TMB} + [TMB]}$$

$$K_m^{TMB} = \frac{K_m^{TMB}[H_2O_2]}{Km^{H_2O_2} + [H_2O_2]}$$

B.2.1. Lineweaver-Burk

The goal is to simulate the Lineweaver-Burk plots for TMB and H_2O_2 following the theory explained previously. This plot is a graphical representation of the Michaelis-Menten equation used in enzyme kinetics [B.5]. The values obtained by increasing the concentrations of both TMB and H_2O_2 can be used to select the experimental concentrations needed to determine the proper protocol of the detection buffer.

B.3 Capture Mechanism Coverage on the Electrode

B.3.1. Theoretical Coverage Calculation and Cyclic Voltammetry Curves

The successful functionalization of surfaces with MCH and the HPPs was a crucial step for our electrochemical biosensor design. In this section, the theoretical aspects, and experimental

approaches for characterizing these components are presented in the context of an electrochemical DNA biosensor.

As mentioned in the report, MCH molecules and HPP are being used for surface modification to form the self-assembled monolayer (SAM). The theoretical coverage of the SAM layer on the gold electrode surface can be estimated using the following formula.

$$\text{Theoretical Coverage} = \frac{\text{Amount of SAM [mol]}}{\text{Electrode Surface Area}[\text{mm}^2]}$$

Another method to assess the theoretical coverage of the SAM layer on electrodes is by cyclic voltammetry, where the surface coverage of the SAM layer can be estimated by comparing the charge during the reduction/oxidation of cyclic voltammetry [B.6]. The following formula can be used:

$$\text{Surface Coverage} = 1 - \left(\frac{Q_{\text{SAM}}}{Q_{\text{bare electrode}}} \right), \text{where } Q \text{ represents the charge}$$

B.3.2. Spectroscopy and Beer's Lamber Law

Spectroscopic methods, such as UV-visible spectroscopy, use Beer Lambert's law to quantify the presence of multiple absorbing species in solution. For HRP-Streptavidin, absorbance (A) can be related to concentration (C) using the following formula:

$$A = \varepsilon \times C \times l$$

Where ε is the molar extinction coefficient, C is the concentration of the absorbing species, and l is the path length of the sample.

B.3.3. Electrochemical Impedance Spectroscopy (EIS)

Electrochemical impedance spectroscopy is a powerful technique that allows sensitive, relatively fast, and quantitative verification of the formation of self-assembled monolayers on the surface of gold screen-printed electrodes, which is crucial for the development of reliable electrochemical biosensors. The formation of SAMs made of MCH on the electrode surface would lead to a ~10-fold decrease in the double-layer capacitance at the electrodes surface compared to the bare gold electrode due to the low dielectric constant of the MCH layer which prevents diffusion [B.7]. On top of this, there is an increase in the charge transfer resistance, or in other words a significant increase in the semicircle in the Nyquist plot.

B.3.4. Scanning Electron Microscopy (SEM)

This high-resolution imaging technique is used for surface imaging to reveal the surface morphology of a material. Thus, it is used to visualize changes in the surface area, helping to determine if there exists a binding of molecules. SEM was used to characterize the functionalization of AuNPs on the screen-printed carbon electrodes.

B.3.5. Dynamic Light Scattering (DLS)

DLS was used to determine the size distribution profile and diameter of the synthesized gold nanoparticles (AuNPs). This technique is sensitive to changes in particle size; thus, it can be used to detect aggregation and changes in particle size over time. Through DLS, the stability of AuNPs was monitored.

B.4. References

- [B.1] S. Ramalingam, A. Elsayed, and A. Singh, “An electrochemical microfluidic biochip for the detection of gliadin using mos2/graphene/gold nanocomposite,” *Microchimica Acta*, vol. 187, no. 12, 2020. doi:10.1007/s00604-020-04589-w
- [B.2] A. R. Arnold, M. A. Grodick, and J. K. Barton, “DNA Charge Transport: from Chemical Principles to the Cell,” *Cell Chemical Biology*, vol. 23, no. 1. Elsevier BV, pp. 183–197, Jan. 2016. doi: 10.1016/j.chembiol.2015.11.010.
- [B.3] A. Abi and E. E. Ferapontova, “Unmediated by DNA Electron Transfer in Redox-Labeled DNA Duplexes End-Tethered to Gold Electrodes,” *Journal of the American Chemical Society*, vol. 134, no. 35. American Chemical Society (ACS), pp. 14499–14507, Aug. 23, 2012. doi: 10.1021/ja304864w.
- [B.4] L. S. A. Busa, M. Maeki, A. Ishida, H. Tani, and M. Tokeshi, “Simple and sensitive colorimetric assay system for horseradish peroxidase using microfluidic paper-based devices,” *Sensors and Actuators B: Chemical*, vol. 236. Elsevier BV, pp. 433–441, Nov. 2016. doi: 10.1016/j.snb.2016.06.013.
- [B.5] M. Li et al., “Multiple effects of sodium dodecyl sulfate on chromogenic catalysis of tetramethylbenzidine with horseradish peroxidase,” *Journal of Dispersion Science and Technology*, vol. 42, no. 4. Informa UK Limited, pp. 526–536, Dec. 19, 2019. doi: 10.1080/01932691.2019.1702050.
- [B.6] Z. Ölcer *et al.*, “Microfluidics and nanoparticles based amperometric biosensor for the detection of cyanobacteria (*Planktothrix Agardhii Niva-CYA 116*) DNA,” *Biosensors and Bioelectronics*, vol. 70, pp. 426–432, 2015. doi:10.1016/j.bios.2015.03.052

[B.7] J. Rivera-Gandía and C. R. Cabrera, “Self-assembled monolayers of 6-mercaptop-1-hexanol and mercapto-n-hexyl-poly(dt)18-fluorescein on polycrystalline gold surfaces: An electrochemical impedance spectroscopy study,” Journal of Electroanalytical Chemistry, vol. 605, no. 2, pp. 145–150, Jul. 2007. doi:10.1016/j.jelechem.2007.03.021

Appendix C: Test Plan for the Constructed Design Prototype

Updates on test plan:

Ideally, some of the tests were planned for a minimum of 3 repetitions. However, we run low on electrodes for testing due to budget and troubleshooting during the fabrication process definition. The number of tests will be detailed in the results document.

Detailed Description of Test Plan

C.1 Primary Requirements

1) Specific to polymorphism CYP2C19*2

To ensure that the GeneDetek biosensor is specific to CYP2C19*2 and CYP2C19*17, we will compare the probe's ability to bind to the target sequence against strands of similar sequences with increasing numbers of mismatches. Significant differences in signals acquired by the transducer can indicate the ability of the probe to bind specifically to the target sequence. Consequently, our probe will be tested against the following DNA sequences: (1) the target sequence, (2) a non-cognate sequence, (3) the target sequence with 1 mismatch, and (4) the target sequence with 2 mismatches.

The baseline targets for passing tests will be set as a ratio between the voltammetry signal produced from certain concentrations of the target analyte and the signal produced from similar concentrations of non-target sequences in a saliva sample. A ratio of 3:1 must be exceeded between the target sequence and a non-cognate sequence. A ratio of 2:1 must be exceeded between the target sequence and the target sequence with 1 mismatch. Furthermore, the target sequence with 2 mismatches must have a smaller signal than the target sequence with 1 mismatch. If these are fulfilled, the DNA bioreceptor probe can be considered specific. Additionally, the degree to which

they are fulfilled will also indicate proportionately the degree to which the probe is specific because of our signal-on design.

CYP2C19*17 is currently not being tested due to budget limitations and the need for contingency in the event that testing does not go as planned for CYP2C19*2. However, considering that the design of the bioreceptor probe is modular, simply swapping the CYP2C19*2 sequence with one corresponding to CYP2C19*17 should work similarly well as their function within the component is the exact same. Therefore, it can be assumed that if the probe for CYP2C19*2 fulfills the tests detailed above, so would a probe for CYP2C19*17.

Objective: Compare the signal ratios of the target sequence to those of the test DNA sequences to determine the specificity of the probe.

Test Procedure:

- Evaluate signal taken from 10 nM of target sequence on the sensor. Take measurements 3+ times (each time washing thoroughly) to acquire the mean signal from target sequence.
- Repeat measurements with 10 nM of test DNA sequence on sensors (taking 3+ measurements).
- Calculate ratios between the target sequence and test DNA to determine test results.
- Ratios must exceed the values detailed above to pass the test and be considered specific



- 3:1 target sequence to non-cognate sequence
- 2:1 target sequence to 1- and 2-mismatch

2) Sensitive to low concentrations

The test plan for evaluating sensitivity to low concentrations of our biosensor will focus on four main performance indicators: 1) signal-to-noise ratio (SNR), 2) limit of detection (LOD), 3) calibration curve, and 4) linearity. The signal-to-noise ratio evaluates the quality of the signal with respect to the background noise. The LOD indicates the lowest concentration that can be reliably detected by our sensor. The calibration curve is needed to find the best-fit function that represents the working range of the biosensor. Linearity shows that the relationship between an increase in concentration with an increase in response is directly proportional. Thus, resulting in accurate quantification of low concentrations.

The target DNA concentrations to obtain the above indicators are: 0nM, 2nM, 4nM, 6nM, and 8nM. These values deviate from the initial customer requirement of <25ng/ml as we are limited by the minimum final yield of Millipore, the company that we are getting our target DNA from. Therefore, Genedetek should detect a target DNA concentration of <10nM to be considered a pass  and this threshold will be considered for the following indicators as well.

2.1) SNR

Objective: Evaluate if the SNR value is high as it indicates reliable and accurate detection.

Test procedure:

- The baseline signal will be measured by using a blank measurement of the nuclease-free water without the presence of the analyte.
- The target signal will be measured using one of the known concentrations used for calculating the calibration curve.
- The SNR value is calculated using the following formula. The ratio is expressed in decibels (dB)

$$\text{SNR} = 20\log(\text{Psignal}/\text{Pnoise})$$

- If the SNR is at least three times higher than the background noise (3:1) it is considered a pass .

2.2) Calibration curve

Objective: Determine the calibration curve of our biosensor to identify the concentration of unknown samples. The calibration curve is also used to determine the LOD.

Test procedure:

- Prepare a stock solution of 8nM of stock DNA.
- Prepare a minimum of five standard solutions with known concentrations if the target DNA using the stock solution
- Use the biosensor to measure the response of each standard solution. In our case, the measurement to be recorded is an amperometric signal or current response.
- Plot the current (uA) vs the known concentrations of the standard solutions.
- Keep the data points that show a linear response and perform a linear regression to find the best fit line or calibration function.
- Obtaining a linear calibration curve is considered a pass .

2.3) LOD

Objective: Determine the limit of detection (LOD).

Test procedure:

- Calculate LOD using the previously derived calibration curve and the following formula:
$$\text{LOD} = 3.3 * (\text{standard deviation of the y-intercept of the regression line})$$
- The expected LOD value should be below 10fM or >3SD for the test to pass .

2.4) Linearity

Objective: Determine the biosensor's linear range of operation.

Test procedure:

- Analyze the residuals in the calibration curve and identify if they behave randomly around zero. If so, the data indicates linearity which is considered a pass 

3) Target to saliva sampling

The current techniques for gene mutation detection rely on extracting blood samples which can be invasive or not applicable for certain patients, whereas relying on saliva would be considered non-invasive and accessible to all patients. Based on this, to verify that our device meets the requirement we would focus on two aspects, 1. the technical feasibility of detecting gene mutations on saliva, and 2. the level of satisfaction of patients with the saliva collection technique. Given that we are still in the Prototyping Phase, we are primarily concerned with feasibility.

Objective: Compare the signal response of target DNA suspended in artificial saliva to the signal response of target DNA suspended in nuclease-free water

Test procedure:

- Synthesize artificial saliva to allow for a controlled introduction of contaminants and introduce different concentrations of target DNA. Such concentrations will be determined from the LOD Test results.
- Measure and compare the signal response between target DNA in artificial saliva and target DNA in nuclease-free water. If the total error is within a tolerance of 10% it will be considered a pass . Protocol for incubation to be determined from Plan for Rapid Testing and Detection Test results.

Note that our initial requirement was to meet >85% agreement rate with a blood-based diagnosis method, however, due to limited resources and time we have identified an earlier level of verification which is the one outlined above (Artificial saliva vs Nuclease-free water).

4) Point-of-Care Design Verification

The following test plan focuses on two procedures to verify that the GeneDetek biosensor has a POC design. The test will focus on evaluating the portability of the device as well as the user interface. A usability test, found in the appendix, combining quantitative and qualitative measures, will be used to assess if the biosensor complies with the requirement of being a POC device.

4.1) Test for Portability and Ergonomics

Objective: Verify that the design is portable and has a user-friendly design.

Test Procedure:

- Evaluate the weight and dimensions of our biosensor(including portable potentiostat):

This will be achieved by measuring and recording the weight and dimensions of the device.

The table below will be used to compare the design's dimensions against the threshold values established in our customer requirements.

Dimensions	Threshold	Measured	Pass  /
Weight	< 20 g		Failure 

Length	< 20 cm		<20 cm Pass <input checked="" type="checkbox"/>
Width	< 20 cm		<20 cm Pass <input checked="" type="checkbox"/>

C.2. Secondary Requirements

1) Rapid Testing and Detection

The following test plan will be used to assess the performance of the GeneDetek biosensor in terms of detection speed and test duration. This test will focus on the incubation time of the hairpin probe and the target DNA at room temperature and the time taken for the overall test readout.

1.1) Measure the Incubation Time of the Hairpin Probe and Target DNA

During incubation, the hairpin probe and the target DNA are mixed and allowed to interact and hybridize if they are complementary to each other.

Objective: To measure the time required for the hairpin probe to hybridize with the target DNA (different concentrations) at room temperature.

Test Procedure:

- Prepare the hairpin probe and different concentrations of the target DNA.
- Set up the incubation chamber for the reaction.
- Mix the hairpin probe and target DNA in the reaction buffer,
- Start the timer and incubate the mixture at room temperature.
- Perform fluorescence measurements at different time intervals, time should be < 24h.

1.2) Reaction Time Assessment

Objective: Ensure that the time taken to collect the sample, prepare the sample, put the sample on the biosensor, and to generate a signal/current is within a 24h time limit.

Test Procedure:

- Measure the time that it takes to collect a saliva sample.
- Measure the time that it takes to prepare the saliva sample.
- Measure the time that it takes to place the specimen on the biosensor, and for it to generate a signal.
- Measure the time it takes to analyze the results.
- Sum the times and validate the time is < 24 hours for the biosensor to pass .

2) Cross-Reactivity

One of the cross-reactivity risks of our sensor could be attributed to obtaining a signal from the enzymatic reaction caused by other factors than the target DNA hybridization. Therefore, we will test hybridization without HRP to better understand the signal magnitude difference. We will use an analysis of variance (ANOVA) statistical test to determine the statistical relevance of this difference. The resultant p-value will be used to determine if the difference in signal is significant. If the p-value is less than 0.05, it would indicate the difference is relevant and it will be considered a pass .

Additionally, saliva is known to contain many different forms of bacterial DNA and contaminants. Budget-allowing, we will introduce further contaminants into our saliva test including alternative forms of DNA from sources commonly found within the oral cavities to better understand how sensitive our device would be in environments where samples are provided that

have not been adequately prepared with a DNA prep kit. Such tests would include similar lab procedures as discussed above in addition to redetermining signal ratios in the midst of severe contaminants.

Objective: Analyze saliva samples with artificial contaminants that mimic a real environment.

Test Procedure:

- Conduct test of signal ratios with target sequence and non-cognate sequences with and without contamination (total 3+ measurements for each study)
- Signal ratios of 2:1 between the target sequence and non-cognate sequences will be considered a pass .

3) Small Sample Volume Compatibility

Our target sample volume is ~5 ml obtained from a saliva spit. The test for small sample volume compatibility will be complementary to the test for sensitivity to low concentrations. To mimic the small sample volume, varying DNA concentrations will be prepared as standard solutions, particularly at very low concentrations. The passing criteria will be consistent with the LOD Test results, where if a test is successful with a target DNA concentration below 10fM it will be considered a pass .

4) Usability and User-Friendly

Objective: Ensure the user interface is intuitive and user-friendly and confirm that the device is easy to use with minimal steps.

Test Procedure:

- Conduct the usability test (qualitative) with a diverse group of potential users. The feedback will be implemented in future iterations of the device.
- The usability test for evaluating that user interface is intuitive and user-friendly will focus on:
 - Evaluating the ease of following the device's operational procedures stated in the instructions manual which is attached in the appendix section.
 - Assessing the complexity of sample collection and preparation.
 - Obtaining feedback on the instructions manual.

4.1) Usability Test for Point-of-Care Design Verification

Objective: The objective of this usability test is to evaluate the user interface intuitiveness, and ease of use of the biosensor for potential users.

Participants: Students representing the intended potential users of the biosensor.

Test Scenarios:

a. User Interface & Ease of Use Assessment:

Task: Provide users with the instructions manual and ask them to collect the sample, start the test, and read and interpret the results.

Data Collection:

- a. Conduct post-task interviews to gather participants' feedback about the biosensor.

Post-task Interview Questions:

Category	Question	Answer	Score
User Interface & Ease of Use Assessment			
Overall Experience	Please rate your overall experience using the biosensor on a scale of 1 to 10 where 1 is extremely poor and 10 is excellent.		$>7 = \text{good}$ $<7 = \text{bad}$
Ease of Use	Please rate how easy it was to read and follow the instructions in the user's manual on a scale of 1 to 10 where 1 is extremely poor and 10 is excellent.		$>7 = \text{good}$ $<7 = \text{bad}$
Sample Collection and Preparation	Please rate how easy it was to collect and prepare the sample on a scale of 1 to 10 where 1 is extremely poor and 10 is excellent.		$>7 = \text{good}$ $<7 = \text{bad}$

Challenges Faced	Were there any challenges or difficulties you faced while using the biosensor? If yes, please briefly describe all the challenges.	1. 2. 3.	
-------------------------	--	------------------------	--

4.2) Instructions Manual

GeneDetek

Standard Test for CYP2C19*2

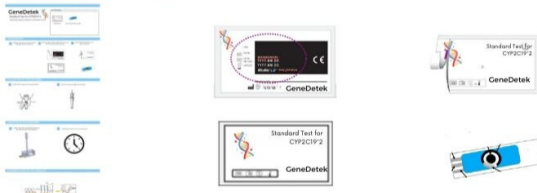
PLEASE READ CAREFULLY BEFORE YOU PERFORM THE TEST

KIT CONTENTS



PREPARATION

- 1 Carefully read instructions for using the Standard Test for CYP2C19*2
- 2 Check the expiry date at the back. Do not use the kit, if expiry date has passed.
- 3 Check that the test device is in good conditions.



COLLECTION OF THE SPECIMEN

- 1 Collect saliva sample into a extraction buffer
- 2 Press the nozzle cap tightly onto the tube.

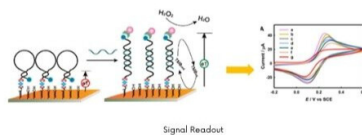


ANALYSIS OF THE SPECIMEN

- 1 Apply a few drops of extracted specimen to the specimen well of the test device.
- 2 Read the test result in 15 min up to 24 hours



INTERPRETATION OF TEST RESULTS



Appendix D: Final Design Specifications

D.1 Hairpin-loop Probe Design.

Initial design plans started with the identification of the sequence for our intended target of interest, CYP2C19*2. This was derived by identifying the following reference SNP cluster identification number (rs ID), *rs4244285*, and determining the base nucleotide substitution between the normal and wild-type alleles which corresponded to a G>A transition [D.1, D.2]. The sequence for the CYP2C19*2 strand was identified by the NCBI databank for SNPs (<https://www.ncbi.nlm.nih.gov/snp/>) by searching for the SNP with the rs ID and selecting the Flanks tab to acquire the nucleotides sequences on either side of the SNP [D.3]. The following is the normal type allele sequence for CYP2C19*2 with its flanking nucleotides on either side [D.3]:

5' – TTCCCACTATCATTGATTATTCGGGAACCCATAACAAATTACTTAAAA – 3'

3' – AAGGGTGATAGTA~~ACTAATAAAGGG~~CCTTGGGTATTGTTAATGAATTT – 5'

The wild-type allele and its complementary sequence are as follows [D.3]:

5' – TTCCCACTATCATTGATTATTCAGGAACCCATAACAAATTACTTAAAA – 3'

3' – AAGGGTGATAGTA~~ACTAATAAAGGG~~TCTTGGGTATTGTTAATGAATTT – 5'

Considering that the probe must be complementary to the wild-type sequence for CYP2C19*2, the complementary strand of the wild-type allele is used to create the loop portion of the hairpin-loop probe. When considering the stability of the hairpin-loop probe, a couple of design considerations were made. Firstly, the length of the loop must be considered as this will affect parameters such as melting temperature and GC% (i.e., percentage of guanine and cytosine). Additionally, a longer loop may provide more chances for secondary structures to form. An ideal length is between 16 to 20 base pairs as the length will ensure selectivity. However, a shorter

length is likely to be preferable for detecting an SNP as it is easier to distinguish a single base pair substitution out of 16 rather than 20 nucleotides.

Secondly, the melting temperature of the beacon must be designed to ensure that the probe stays in its proper conformation within the temperatures of the biosensing system. A melting temperature around 10 °C higher than the maximum temperature of the system it will be placed in is preferable to ensure optimal performance [D.4]. Considering that our current biosensor design is trying to avoid the use of PCR, our sensing system will likely only be required to operate at room temperature or below. However, higher melting point temperatures correlate to greater stability due to higher GC% content so an ideal temperature is somewhere between 65 to 75 °C.

Thirdly, stem design is an integral part of controlling the overall GC% and melting point of the hairpin loop because it is mostly composed of GC base pairs that can be adjusted to achieve the optimal probe parameters. Stem length is usually longer than 3 base pairs and the entire loop of the probe should ideally be more than twice the length of the stem [D.5]. Longer stem lengths correlate to greater stability and specificity but at the cost of the rate of hybridization between the loop and target SNP. However, since our biosensor design is aiming for high specificity and selectivity towards CYP2C19*2, the option for a longer stem is preferable.

Finally, secondary structures should be taken into account as they can introduce non-specific binding and also interfere with the hairpin loop's ability to change conformation when hybridizing with its complementary strand. There are multiple software available for checking secondary structures within a sequence. The following is a free software (<http://biotools.nubic.northwestern.edu/OligoCalc.html>) that provides information on the number of secondary structures in a given sequence and initial specifications such as the minimum and maximum number of base pairs required for self-dimerization and hairpin-loop formation,

respectively [D.6]. Once calculated, hairpin-loop formation is displayed in a list with potential secondary structures outlined in red. In the following figure, the SNP and one base pair on either side are highlighted in yellow.

Figure D.1. Potential HPP secondary structures. Secondary structures are outlined in red with the SNP and flanking base pair on either side highlighted in yellow [D.6]. 50 flanking nucleotides on either side of the SNP are displayed and retrieved from the NCBI SNP databank.

With all these considerations taken into place, the selection of potential hairpin-loop probe formations can be considered. The main factors that have the most weight in selecting a hairpin-loop probe design are as follows (from most important to least important): (1) Secondary Structures, (2) Loop Length, (3) Stem Design, and (4) Melting Temperature.

Hairpin-loop Probe Options.

Three potential hairpin-loop probes were examined for their potential use in our electrochemical biosensor. The following details the reasoning for why our final hairpin-loop probe was selected and how it was validated and adjusted.

Hairpin-loop Probe Secondary Structures Evaluation.

When selecting the loop portion of the hairpin-loop design, initially the length was considered to be 20 base pairs long to ensure selectivity. A couple of secondary structures were noted to have the potential to interfere with the loop portion as shown in Figure D.2.

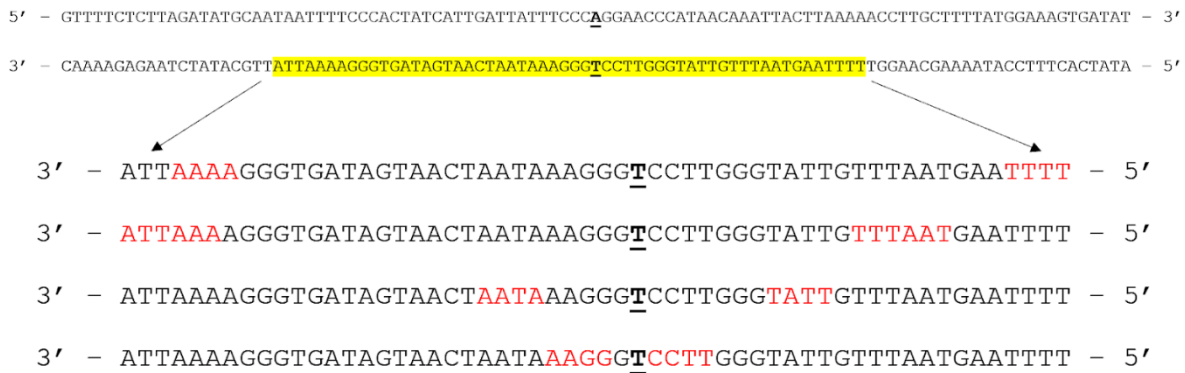


Figure D.2. Potential secondary structures within the yellow highlighted portion of the complementary strand to the target CYP2C19*2 wild-type allele sequence.

The most notable of the two secondary structures is the one directly flanking the SNP that could potentially cause issues in our hairpin-loop structures since the loop would bind to itself making a linear conformation with few base pairs constituting the loop portion. As noted before, this would likely affect the hairpin-loop's ability to change conformation upon hybridization of the target SNP which would reduce the efficacy of the probe. Three potential hairpin-loop structures were considered based on the presence of the probe characteristics and secondary structures that can be seen in the highlighted portions of Figure D.3.

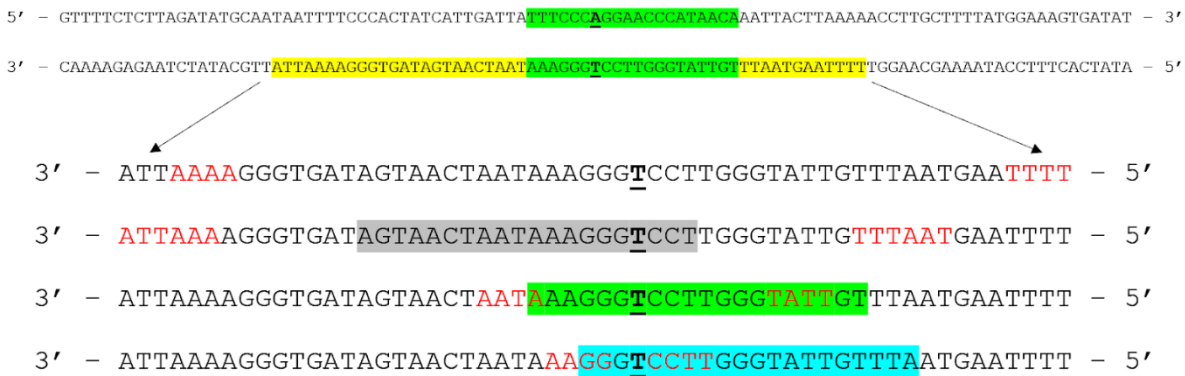


Figure D.3. Three potential hairpin-loop probe formations are highlighted in gray, green, and blue. The respective location of the green probe is displayed in the longer sequence of the CYP2C19*2 allele and the yellow highlighted portion displays the section of the allele that was examined for secondary structures.

Hairpin-loop Probe Characteristics and Comparisons.

All three hairpin-loop probes (identified as gray, green, and blue probes) were examined for their melting temperature and GC content. Additionally, a general approach to the stem portion of the hairpin structure (i.e., 3'-GGCGCC-Loop-GGCGCC-5') was taken by applying the same sequence of guanines and cytosines. The specific sequence was selected to ensure that the GC% was around 60% and the melting temperature was around 70 °C for all three probes. However, higher values were preferred.

Table D.1. Characteristics of melting temperature, GC content, and length for all three probes.

Hairpin-loop Probe	Melting Temp. (°C)	GC Content (%)	Length (bp)
Gray	68.2	59	32

Green	70.8	66	32
Blue	70.8	66	32

The gray hairpin-loop probe has the SNP positioned closer to its 5' side and has no potential hairpin structures of 4 base pairs or longer in length. It has the lowest melting temperature and GC content of the three probes. The green hairpin-loop probe has the SNP positioned closer to the middle of the loop but has a major hairpin loop structure flanking either side of the SNP. The blue hairpin-loop probe has the SNP closer to its 3' side and has no significant hairpin structures. It has the same melting temperature and GC content as the green hairpin-loop probe.

With these characteristics taken into account, the best probe option from the available selection is the blue hairpin-loop probe. A virtual meeting with Professor Juewen Liu (University of Waterloo) was organized to verify the final design of our probe and acquire feedback on how to improve it. One change to our final design based on feedback included the shortening of the loop portion to 17 bp to increase the specificity of the design towards the single nucleotide substitution. This led to a 68.8 °C melting temperature, 65.5% GC content, and 29 bp length.

5' - CCCAGGAACCCATAACA - 3'

3' - CCGCGTGGGTCCTTGGGTATTGTACGCGG - 5'

Final hairpin-loop design and synthetic DNA sequences for testing.

The final hairpin-loop design will require functionalization of both ends of the probe with biotin at the 5' ends and thiol-linker on the 3' end to enable detection of the HRP-streptavidin complex and to allow formation of the SAM on the electrode surface, respectively.

5' - BTN - GGCGCATGTTATGGGTTCCCTGGGTGCGCC - thiC6 - 3'

Our electrochemical biosensor will be tested under the following circumstances (finances permitting):

Table D.2. Oligomer names and test sequences. The underlined nucleotide corresponds to the SNP and the bolded nucleotides correspond to mismatches.

Oligomer Test Name	Oligomer Test Sequence
Target SNP	CCCAGGAACCCATAACA
Blank	-
1 mismatch	CCCAGGAACCCATAACT
2 mismatches	CCCAGGAACCCATT <u>AGA</u>

The target SNP is the exact CYP2C19*2 sequence that we are targeting for our electrochemical biosensor. In the event that this sample is placed on our sensor, it should hybridize with the hairpin-loop probes to begin the sequence of events that will lead to signal generation, verifying that our biosensor can actually detect our target. The subsequent oligomers to be tested will verify that our biosensor is specific and selective to our target sequence. The blank test should not produce any significant signal production when placed on the sensor as it does not have any significant complementary portions to the hairpin-loop probe. If this test generates no significant signal changes, it will verify that the hairpin-loop probe is specific to the target sequence. The mismatch oligomers will verify that the hairpin loop can selectively determine the correct SNP. In general, any mismatch should prevent significant signal generation from occurring. However, with each additional mismatch, any additional signal generation that could occur should be reduced.

D.2 SAM Design

The SAM design originated from a reference paper using a similar thiol-linkage method onto a gold electrode surface [D.7]. Ideally, this design takes advantage of the thiols affinity to bind with gold surfaces to form a natural monolayer of alkanethiols and probes. By modulating the concentration of alkanethiols to probes, this can increase the capture efficiency of the electrode surface with respect to target analyte by decreasing the amount of steric hindrance felt by the HPPs. When HPPs are too close together, they may interfere with each other which may affect hybridization.

The specific fabrication of the SAM utilized 6-mercaptophexanol with thi-C6 modified HPPs. The alkanethiol chain length was selected to match the chain length of the thiol modification on the HPP. This enabled the probes to sit above the monolayer where they could interact with target sequences and hybridize. When in their loop conformation, the probe's biotin was hidden within the SAM layer to prevent binding of HRP-streptavidin. However, when hybridization occurred, the biotin was exposed allowing the binding of HRP-streptavidin as seen in the following figure:

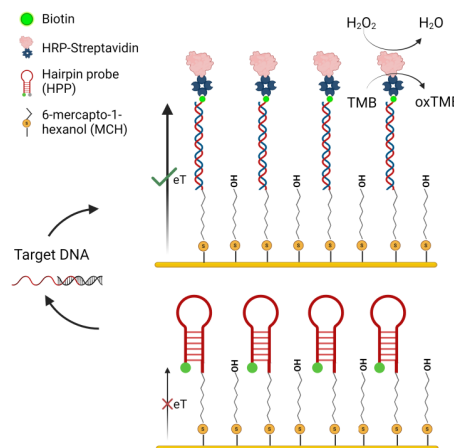


Figure D.4. HPP in closed loop conformation with a hidden biotin molecule. HPP in an open duplex conformation with an exposed biotin molecule.

The exact concentration on the electrode surface was determined by the concentration used to incubate the surface of the electrode and the amount of incubation time spent. Ideally, higher concentrations utilized lower incubation times. The exact final concentration of MCH and HPP used was 10 mM for 20 minutes and 1 uM for 1.5 hours, respectively. This was determined through the generation of calibration curves tested at different concentrations of MCH and HPP.

Characterization of the SAM layer was done using CV and impedance values taken after each step in the deposition method. This was to ensure that each step in the SAM fabrication procedure was working as intended. The principle behind CV is that as a layer is formed on the surface of the electrode impedance increases which reduces the signal of the CV curve. This is due to the fact that electron exchange between the buffer and electrode surface is now impeded by layer of molecules functionalized to the surface. Therefore, as the SAM is fabricated and both components are added to the surface, CV and impedance should have an inverse relationship, see Figure D.5.

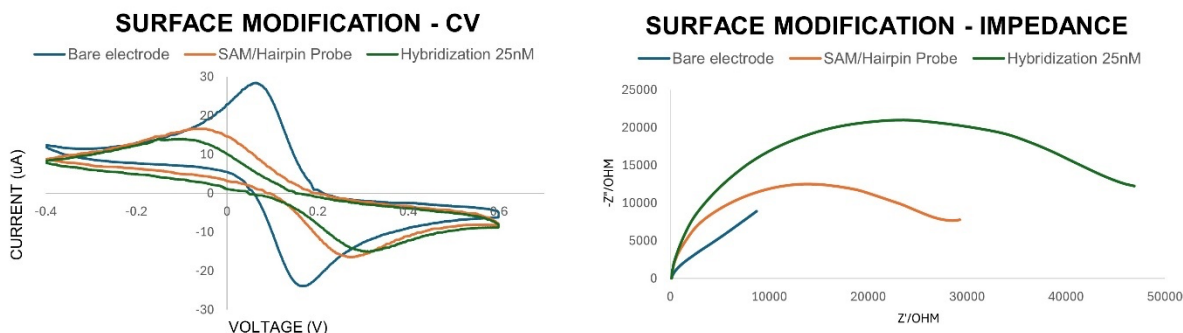


Figure D.5. Verification of surface functionalization with CV (left) and EIS (right)

This inverse relationship is seen in the two characterization methods shown above. The blank electrode has the highest CV signal and the lowest impedance. As the SAM is formed, the

CV signal decreases and impedance increases. This was used to validate the formation of the SAM on the surface of the electrode.

D.3 Transducer and Redox Reactions

Transducer

Our design uses electrochemical transduction for signal interpretation. Electrochemical detection principles use electrodes (conductor or semiconductor) along with detection tools to measure an electrical signal [D.8]. This signal is generated from the interaction between the target analyte and the electrochemical label [D.8]. Our design uses the universal setup for electrochemical measurement. It consists of three electrodes: working electrode (WE), reference electrode (RE), and counter electrode (CE) as seen in Figure D.6.

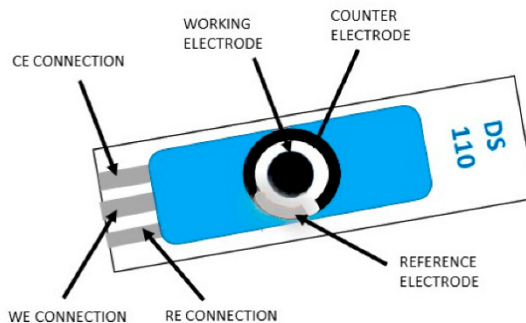


Figure D.6. Commercial screen-printed electrode.

The signal and any enhancement mechanisms should happen on top of the WE. For the RE and CE, common materials will be used. The RE material consists of Ag/AgCl and the CE consists of platinum. The use of standard materials will enhance the stability of the signal processing. However, different WE materials have been considered to meet our customer requirements within the available resources for the project. This includes:

- 1) Screen-printed carbon electrode

- 2) E-beam gold electrode
- 3) Screen-printed carbon electrode modified with AuNPs

Of the materials considered, the majority of our experiments have been conducted on screen-printed gold electrodes functionalized through our protocols. While screen-printed carbon electrodes modified with AuNPs were considered and characterized in the early stages of testing, it was observed that the AuNPs had aggregated on the surface of the electrodes and produced uncharacteristic CV and impedance results. This introduced additional variability into our tests so it was decided to not continue official testing with screen-printed carbon electrodes modified with AuNPs. Additionally, screen-printed carbon electrodes were considered due to their cost-effectiveness. However, since our main principle of operation for the SAM involved the thiol-linkage using a gold electrode surface, screen-printed carbon electrodes were not used.

Redox Reaction

The redox reaction involving the use of HRP, TMB, and hydrogen peroxide is used to generate the necessary change in charge on the electrode surface to produce a signal. This is employed through the oxidation of TMB. Ideally, HRP's redox site centrally located within the macromolecule and the TMB redox molecule is utilised as an electron shuttle that can penetrate both HRP and the SAM. This enables exchange of electrons at the electrode surface. Through the reduction of hydrogen peroxide with TMB on the electrode surface, a signal can be generated [D.7]. The following schematic details the reaction between TMB and hydrogen peroxide in the presence of HRP:

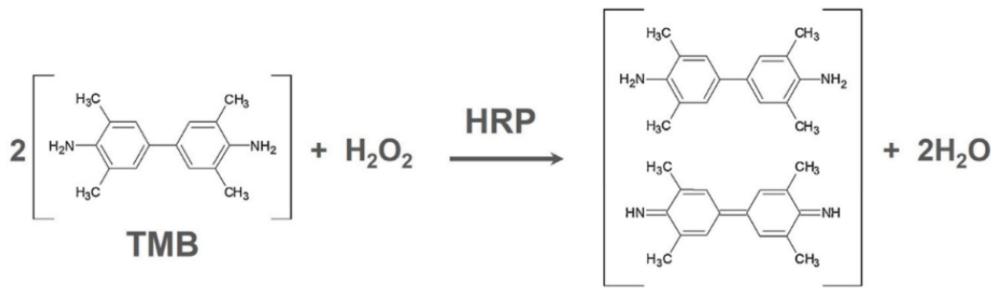


Figure D.7. Redox reaction of TMB with hydrogen peroxide in the presence of HRP [D.10].

D.4 Software Application

The software application developed to interpret the results of the biosensor can be found at the following link: <https://genedetek.streamlit.app/>. The application was built in python and generates a report of the results taken from a potentiostat and interprets them in a user-friendly manner. Additionally, this application cross-references the signal generated to the concentration of target analyte by utilising the calibration curve developed in prior in-lab experiments. The end result of this application outputs a report that indicates a positive or negative result and the corresponding drugs that are associated with the affected gene mutation.

The python code used to create the app can be found in: [GitHub Repository](#). The app serves as an interface for processing and visualizing the collected data, as well for generating diagnostic reports. The libraries used to write the code were NumPy, Pandas, Matplotlib, and SciPy. The `read_calibration_curve_csv` function within the code reads calibration data from a CSV file, while the `create_calibration_function` employs linear regression to interpolate the calibration data, establishing a function that correlates current response with analyte concentration. Users can upload CSV files generated by the potentiostat; the script processes these files to identify the

maximum current and, against a calculated Limit of Detection (LOD), determines if the result is "positive" (above LOD) or "negative" (below LOD).

D.5 SolidWorks Encasing Design

The 3D model of the encasing was designed using SolidWorks. Figure D.8 represents a schematic of the design along with its final dimensions. Subsequently, the encasing was fabricated with a MK3S+ Prusa 3D printer. Polyethylene Terephthalate (PTE), known for its light weight, was the material used for 3D printing. The final 3D printed model had the following dimensions: a length ~ 3.2 cm, a width of 4.0 cm, and a weight of 10.68 g.

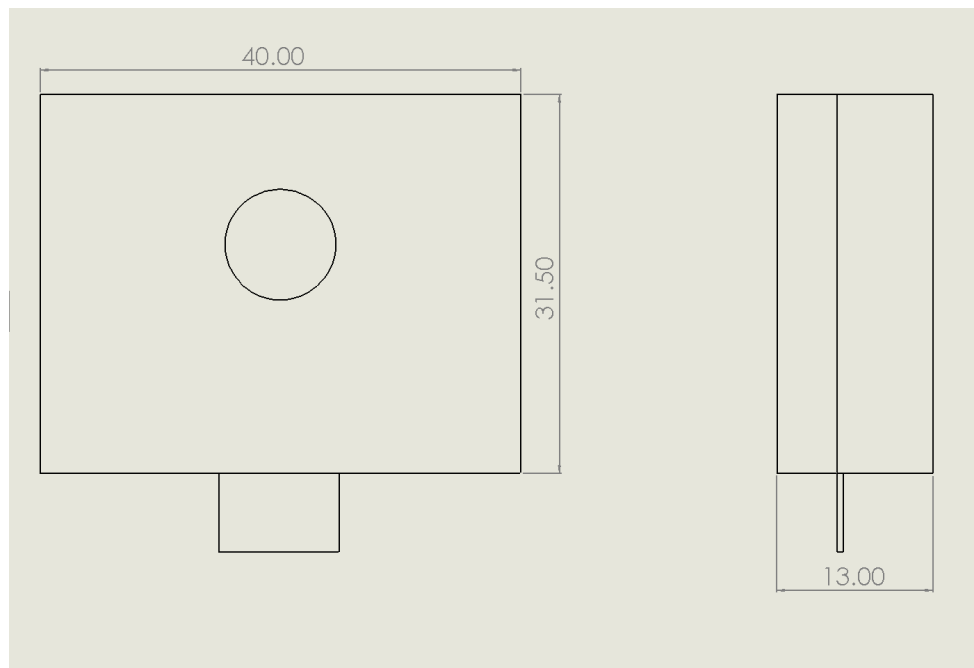


Figure D.8. SolidWorks Sketch Dimensions

D.6 Fabrication Protocol

The following details the protocol for fabricating one screen-printed gold electrode.

Cleaning (~20 minutes):

- 1) Clean with Millipore water and dry with nitrogen gun.

- 2) Add ~120 μ L of 0.1M H₂SO₄ over all three electrodes and run CV with the following parameters:
 - Init and Low E (V): 0.0
 - High E (V): 1.3
 - Polarity: Positive
 - Scan Rate (V): 0.1
 - Sweep Segments: 40
 - Interval: 0.001
 - Quiet Time: 2
 - Sensitivity: 1e-004
- 3) Use pipette to absorb H₂SO₄ and place it back to the 0.1M H₂SO₄ vial.
- 4) Clean electrode with millipore water and dry with nitrogen gun.

HPP Incubation (~1.5 hours):

- 1) Drop cast ~20 μ L of 1uM of HPP in the working electrode's surface (middle circle, avoid touching the other electrodes) and incubate for 1.5h in a covered petri dish at room temperature in the drawer.
- 2) In the fumehood, rinse at least three times with ~1000uL of 1x PBS. Hold the electrode with tweezers or fingers (making sure to not touch the middle circle) at an angle on top of the waste bottle, pipette slowly.
- 3) Dry by carefully tapping the electrode with a kimwipe until it looks dry (making sure to not touch the WE area). If a few drops are left, let it sit for a few minutes until it evaporates.

MCH Incubation (~20 minutes):

- 1) Drop cast ~20 uL of 10mM MCH in the working electrode's surface and incubate for 20mins at room temperature and leave it in the fumehood in a closed petri dish.
- 2) In the fumehood, rinse at least three times with ~1000uL of 1x PBS. Hold the electrode with tweezers or fingers (making sure to not touch the middle circle) at an angle on top of the waste bottle.
- 3) Dry by carefully tapping the electrode with a kimwipe until it looks dry (making sure to not touch the WE area). If a few drops are left, let it sit for a few minutes until it evaporates.
- 4) Rinse at least three times with ~1000uL of 1x PBS. Hold the electrode with tweezers or fingers (making sure to not touch the middle circle) at an angle on top of the waste bottle, pipette slowly.

Hybridization (~1 hour):

- 1) Deposit a ~20 μ L droplet, with various concentrations of target DNA on the WE and keep at room temperature for 1h in the drawer.
- 2) Rinse electrodes two times with ~1000uL of washing buffer.
- 3) Rinse electrodes one time with ~1000uL of 1x PBS.
 - a. For MCH of 10mM, rinse three times with 1000ml of 1xPBS
- 4) Dry by carefully tapping the electrode with a kimwipe until it looks dry (making sure to not touch the WE area). If a few drops are left, let it sit for a few minutes until it evaporates.

HRP Amplification (~30 minutes):

- 1) Deposit ~20 μ L of 1:30 HRP-STV on the WE and keep at room temperature for 30min.
- 2) Rinse electrodes two times with ~1000uL of washing buffer.
 - A. Dispose in HRP waste
- 3) Rinse electrodes one time with ~1000uL of 1x PBS.

A. Dispose in HRP waste

Signal Readout (~5 minutes):

- 1) Deposit ~120 μ L of 0.2mMTMB/10mMH₂O₂ buffer covering all electrodes
- 2) Take measurement with the potentiostat:
 - A. Chronoamperometry
 - B. Cyclic Voltammetry
 - C. Differential Pulse Voltammetry
 - D. Square Wave Voltammetry

Disposal (~5 minutes):

- 1) Rinse electrodes with millipore water and dispose of waste in the HRP waste container.

References

- [D.1] "rs4244285." PHARMGKB. <https://www.pharmgkb.org/variant/PA166154053>.
- [D.2] M. Dehbozorgi, B. Kamalidehghan, I. Hosseini, Z. Dehghanfar, M. H. Sangtarash, M. Firoozi, F. Ahmadipour, G. Y. Meng, and M. Houshmand. "Prevalence of the CYP2C19*2 (681 G>A), *3 (636 G>A) and *17 (-806 C>T) alleles among an Iranian population of different ethnicities," NIH, vol. 17, no. 3. Mol Med Rep, pp. 4195-4202, 2018. doi: 10.3892/mmr.2018.8377.
- [D.3] "RS4244285 RefSNP report - dbSNP - NCBI," National Center for Biotechnology Information, <https://www.ncbi.nlm.nih.gov/snp/rs4244285#flanks> (accessed Dec. 4, 2023).
- [D.4] "Molecular Beacon Documentation," Purdue iGEM, 2020. <https://static.igem.org/mediawiki/2021/5/54/T--Purdue--Beacon-Doc.pdf>.
- [D.5] S. Tyagi, and F. R. Kramer. "Molecular Beacons: Probes that Fluoresce upon

Hybridization,” Nat. Publishing Group, vol 14, Nat BioTech, pp. 303-306, 1996.

[D.6] Q. C. Warren Kibbe, “Oligo Calc: Oligonucleotide properties calculator,” OligoCalc: Oligonucleotide Properties Calculator, <http://biotools.nubic.northwestern.edu/OligoCalc.html> (accessed Dec. 4, 2023).

[D.7] G. Liu et al., “An Enzyme-Based E-DNA Sensor for Sequence-Specific Detection of Femtomolar DNA Targets,” Am. Chem. Soc. vol. 130, no. 21, pp. 6820-6825, Jan. 2008. doi: 10.1021/ja800554t.

[D.8] K. T. Kim and N. Winssinger, “Enhanced SNP-sensing using DNA-templated reactions through confined hybridization of minimal substrates (CHOMS),” Chemical Science, vol. 11, no. 16, pp. 4150–4157, 2020. doi:10.1039/d0sc00741b

[D.9] G. Liu et al., “An Enzyme-Based E-DNA Sensor for Sequence-Specific Detection of Femtomolar DNA Targets,” Journal of the American Chemical Society, vol. 130, no. 21. American Chemical Society (ACS), pp. 6820–6825, May 01, 2008. doi: 10.1021/ja800554t.

[D.10] L. S. A. Busa, M. Maeki, A. Ishida, H. Tani, and M. Tokeshi, “Simple and sensitive colorimetric assay system for horseradish peroxidase using microfluidic paper-based devices,” Sensors and Actuators B: Chemical, vol. 236. Elsevier BV, pp. 433–441, Nov. 2016. doi: 10.1016/j.snb.2016.06.013.

Appendix E: Verification Data

E.1 Results of HPP Simulations

The OligoAnalyzer™ tool (<https://www.idtdna.com/calc/analyzer>) by Integrated DNA Technologies (IDT) was used to simulate potential secondary oligonucleotide folding formations for the hairpin-loop probe and the three test DNA sequences. The tool provides quick access to UNAFold - a DNA folding software (<http://www.unafold.org/mfold/applications/dna-folding-form.php>), self/hetero-dimer tools, NCBI Blast, and TM Mismatching to aid in the design of oligonucleotides. See the following table for a general overview of the properties for each sequence of oligonucleotides given:

Table E.1 Parameters of HPP (including modifications), target sequence, mismatch-1 sequence, and mismatch-2 sequence. Information includes length of sequence, GC content, melting temperature, and molecular weight.

	HPP	Target DNA	Mismatch-1	Mismatch-2
Length	29	17	17	17
GC (%)	65.5	52.9	52.9	52.9
T_m (°C)	68.8	51.2	50.9	50.6
MW (g/mol)	9610.5	5117.4	5108.4	5148.4

1) Secondary Structure Analysis

The following details the secondary structures for the HPP and test sequences:

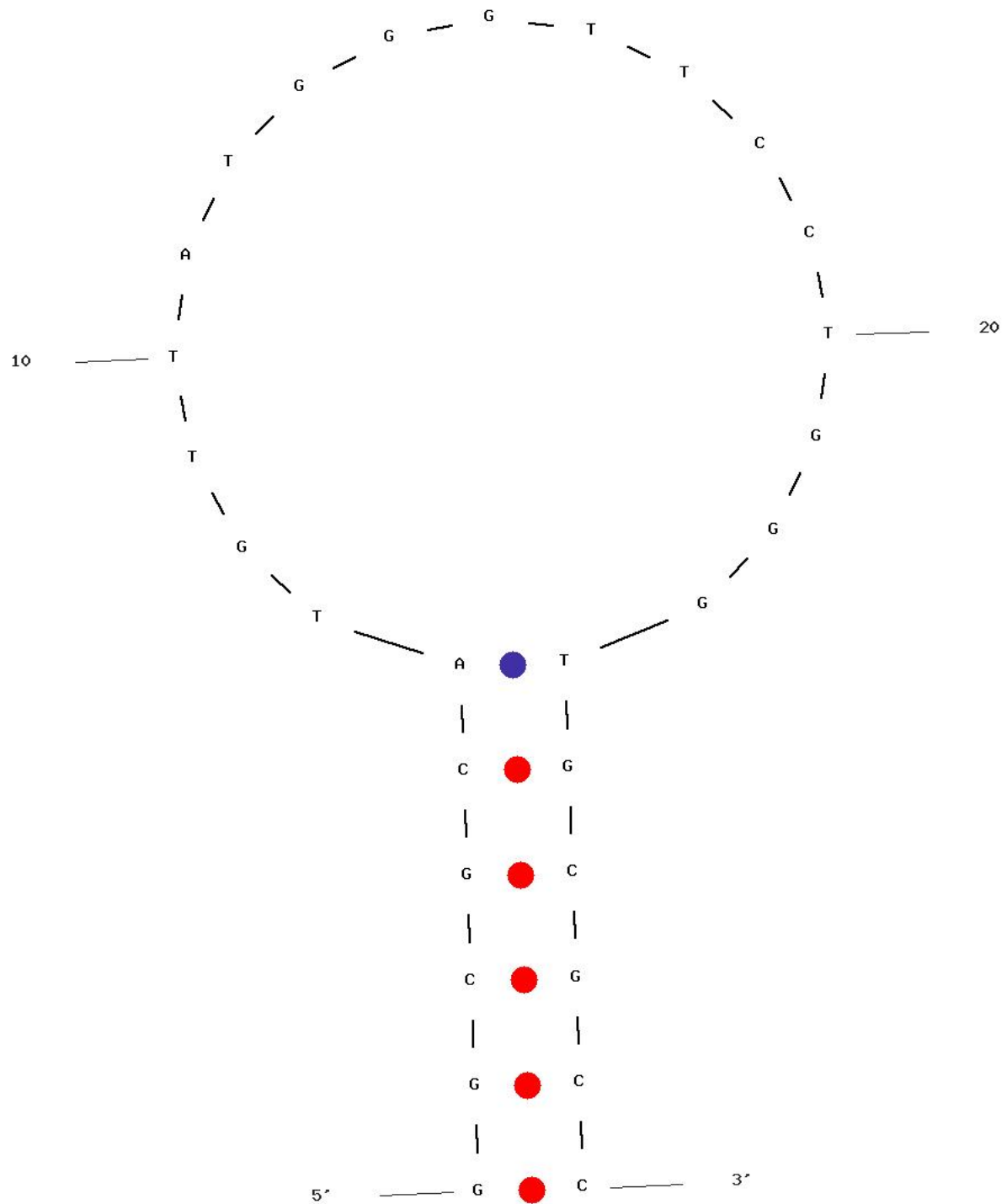


Figure E.1. Formation #1 of hairpin-loop probe (the optimal formation) [E.1].

MFOID_UT11 4.7

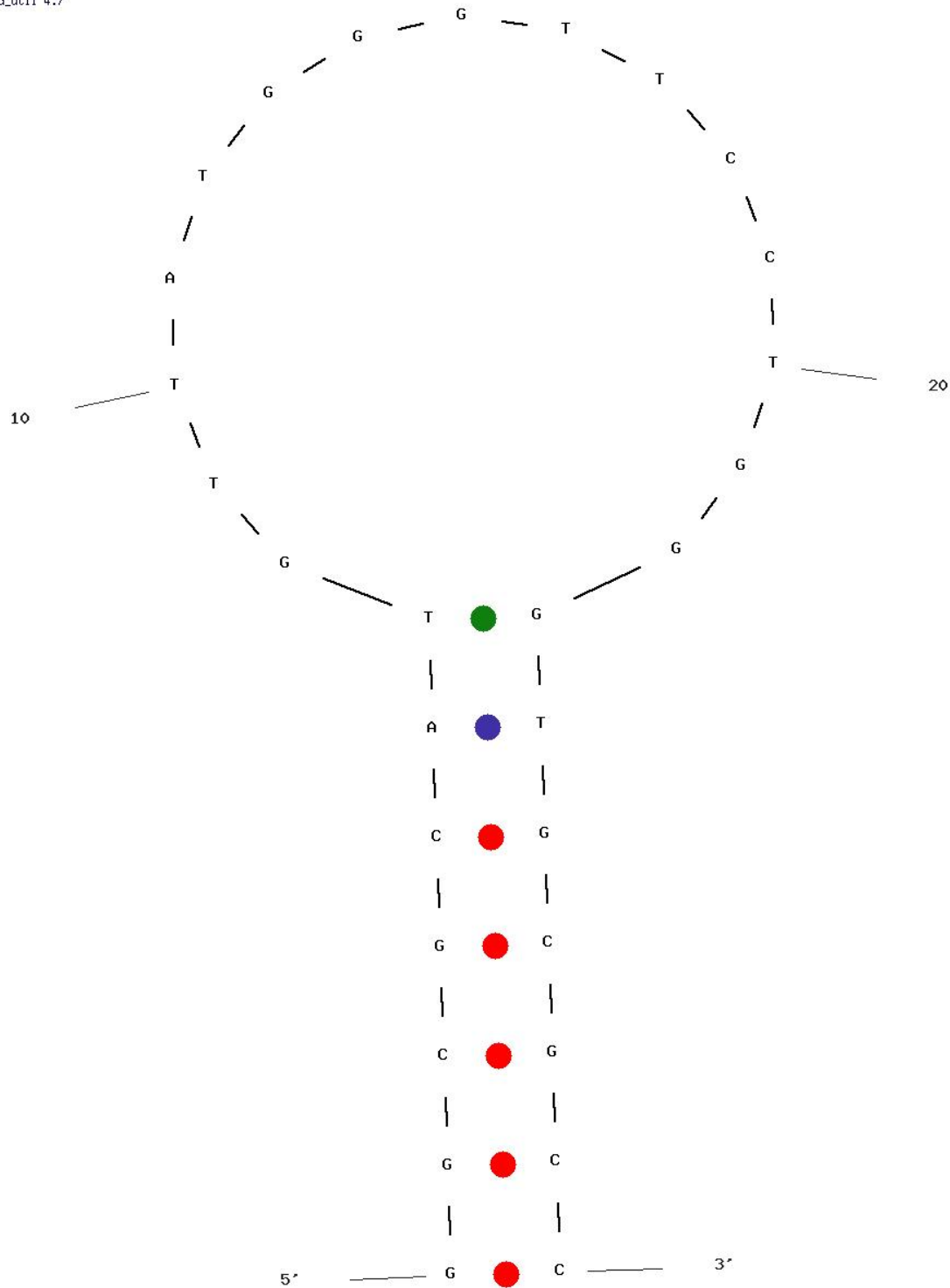


Figure E.2. Formation #2 of hairpin-loop probe with mismatched base pairing of T and G in the stem region [E.1].

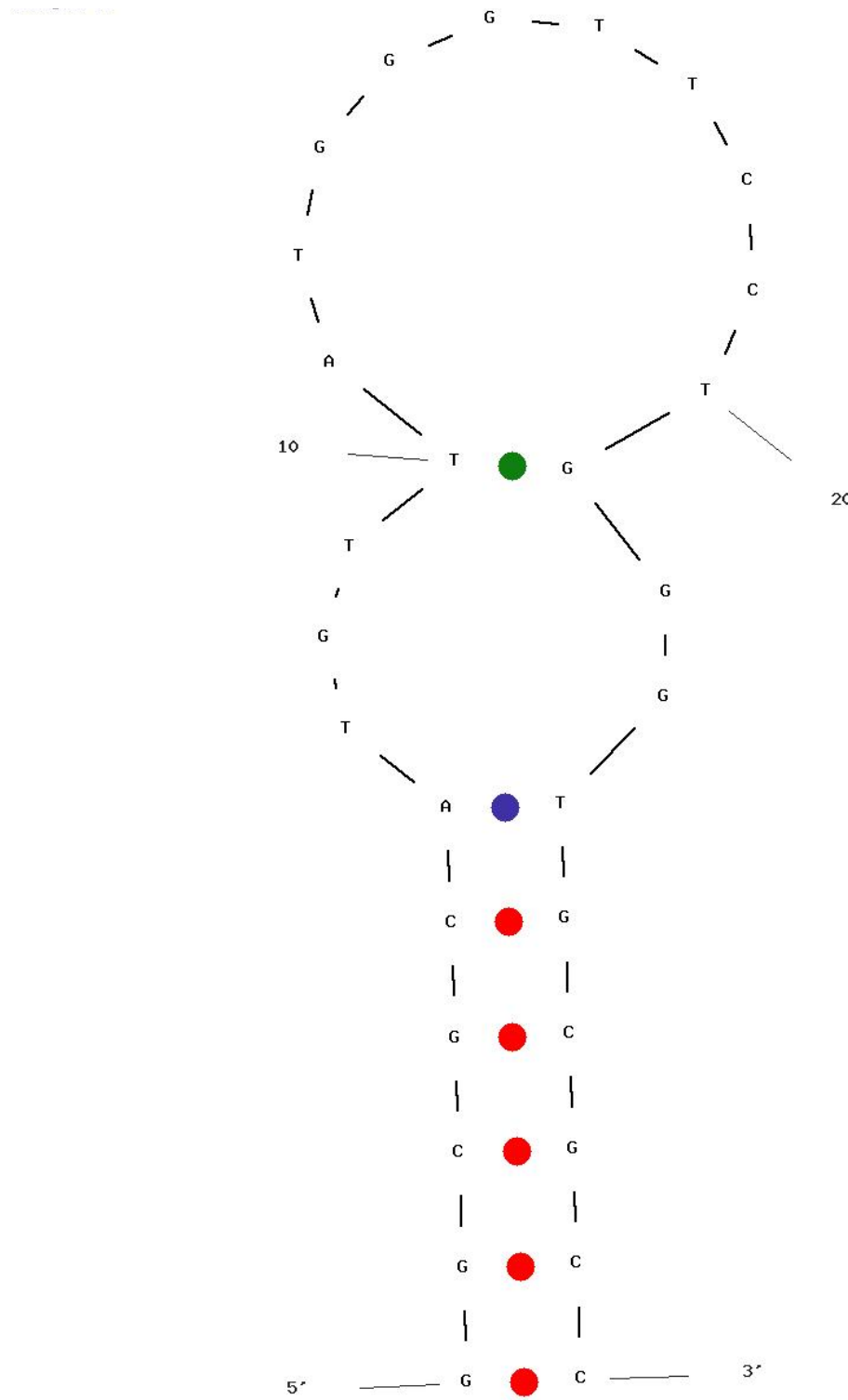


Figure E.3. Formation #3 of hairpin-loop probe with secondary structure formed through mismatched pairing of T and G in the middle of the loop [E.1].

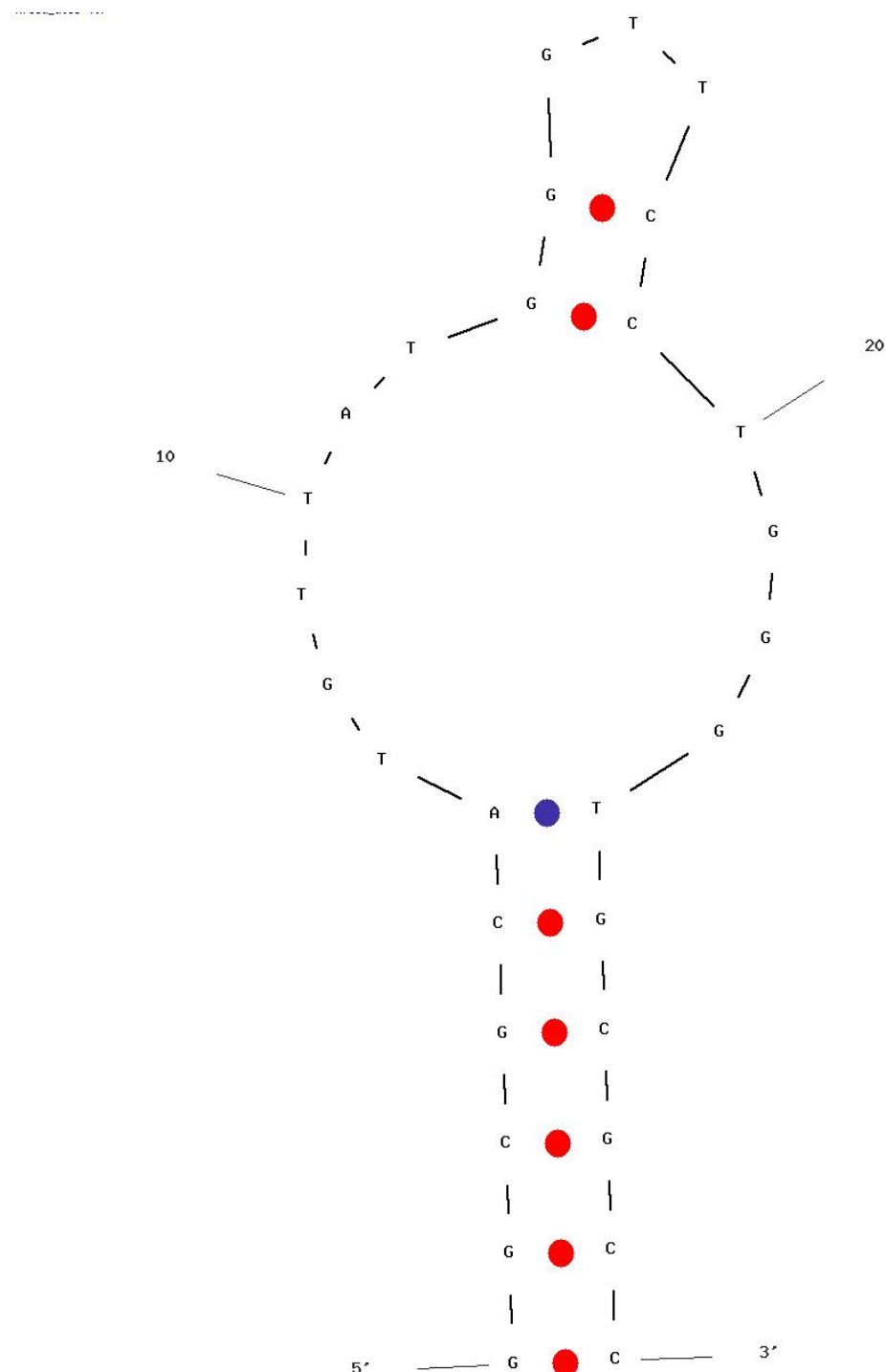


Figure E.4. Formation #4 of hairpin-loop probe with secondary structure formed through the pairing of two base pairs to form another loop [E.1].

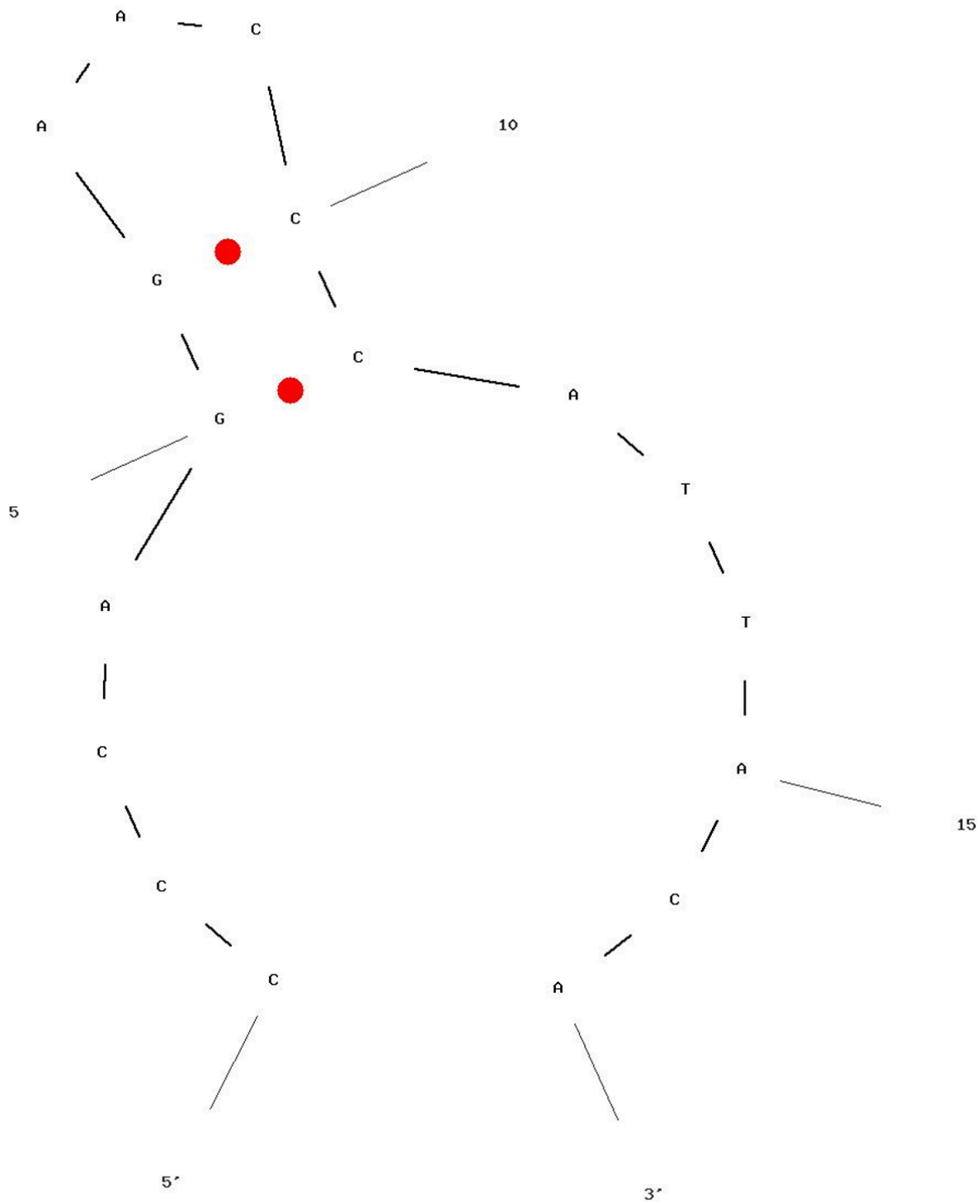


Figure E.5 Formation #1 of test structures with secondary structure forming a hairpin-loop through the pairings of two GC bases [E.1].

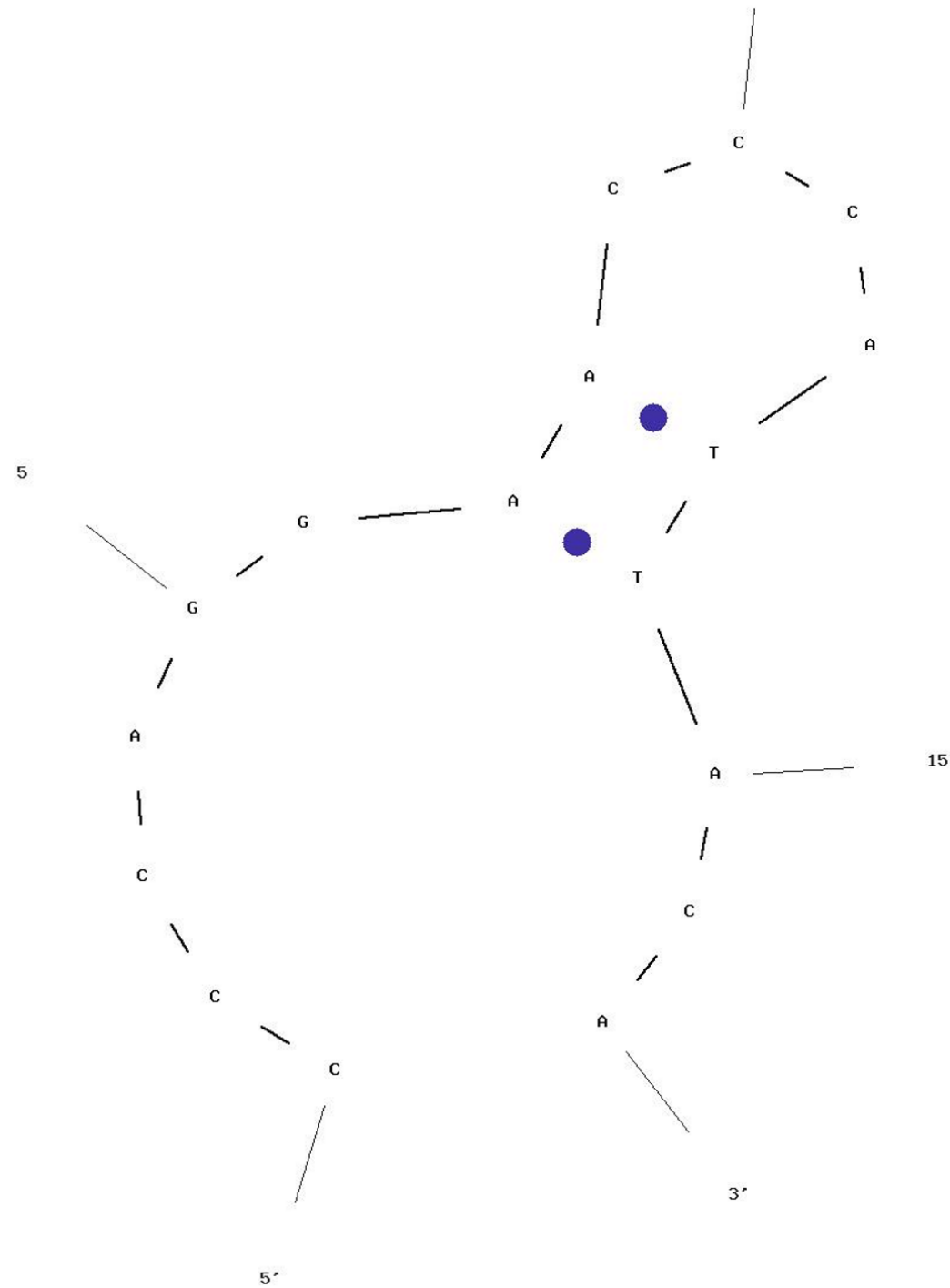


Figure E.6 Formation #2 of test structures with secondary structure forming a hairpin-loop through the pairing of two AT bases [E.1].

2) Thermodynamic Analysis of HPP

Free energy calculations are used to predict the most stable secondary structures that are likely to occur at a given temperature. These values are derived by using the nearest-neighbor thermodynamic parameters published by the following laboratory (Allawi,H., SantaLucia,J.,Jr., Biochemistry, 36, 10581). See the following table for thermodynamic properties of potential hairpin-loop probe formations (see the above figures for hairpin-loop formation and test sequence formation images corresponding to the thermodynamic properties):

Formations	ΔG (kCal/mole)	T (°C)	ΔH (kCal/mole)	ΔS (cal*K/mole)
1	-5.63	62.6	-50.2	-149.5
2	-5.38	61.6	-49.2	-146.96
3	-3.2	43.6	-54.5	-172.07
4	-3.08	40.2	-63.5	-202.64

Table E.2. Secondary structures thermodynamic properties for the hairpin-loop probe [E.1].

Formation 1 is the intended hairpin-loop formation for the oligonucleotides and will provide the optimal structure to bind with the complementary strands. Formation 2 has an additional base pairing in the stem portion that seems to occur due to close proximity of the two bases. Additionally, the two bases are not complementary to each other so this mismatch may reduce the probability of this structure forming. Formation 3 and 4 have unfavourable secondary structures forming in the loop portion of the probe that may interfere or block complementary strands from forming. However, these structures are less stable and have a smaller chance of occurring.

A simple interpretation of these values is that the Gibbs free energy is a good predictor of the probability that a formation will exist. The lower the Gibbs free energy, the more likely that structure will occur. As such, formation 1 and 2 are most likely to exist at room temperature (25 degrees Celsius, the temperature these values were calculated at) whereas formations 3 and 4 are less likely to exist.

However, a few assumptions can be made such that the different folding formations can be interpreted as energy states with their specific energy assumed to be similar to the Gibbs free energy given in the table above. Under these premises, a Boltzmann's distribution can be used to roughly predict the probability of the amount in which each of these four formations will co-exist at a given temperature.

The probability distribution (π_i) is determined by the probability of a single state under a certain energy (e_i) and temperature (T) with respects to the entire system of states (Q) - which can also be called the canonical partition function. K in this instance is the Boltzmann's constant. By calculating the probabilities of the four formations existing at certain temperature intervals, the following profiles are found:

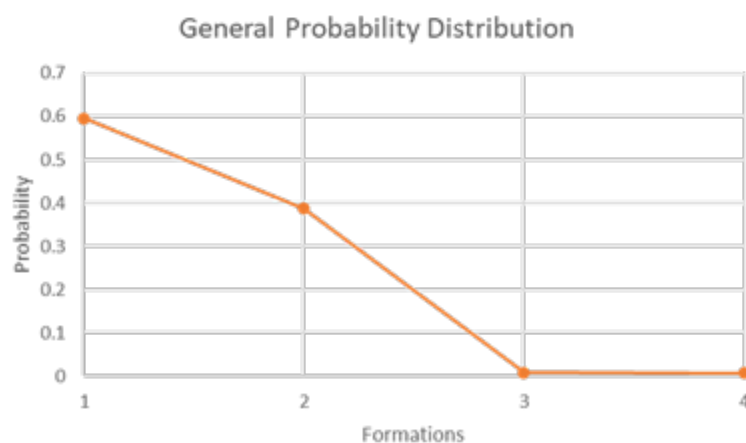


Figure E.7. General probability distribution of hairpin-loop formations at room temperature.

A few assumptions must also be made when interpreting these results. Firstly, the melting point temperature for these structures is around 52 °C on average so we should assume that these probability values are only applicable to oligonucleotides that have actually formed the hairpin-loop structure (i.e., the percentage that actually form hairpin-loop structures will significantly decrease after 52 °C). Secondly, these calculations are also based on assumptions made on comparing the formations to energy systems and are roughly determining the probability that a certain amount of each formation will exist at a given temperature.

It is shown that around 60% of oligonucleotides in their hairpin-loop structure are likely to be Formation 1 and around 40% are likely to be Formation 2. An insignificant amount (<1%) of oligonucleotides will take the Formation 3 and 4 structure at a given temperature. These results are optimal for our applications and prove that a significant amount of our hairpin-loop probes will be in their intended conformation. However, future steps can be taken to experimentally determine these values.

3) Thermodynamic Analysis of Test Sequences

Formations	ΔG (kCal/mole)	T (°C)	ΔH (kCal/mole)	ΔS (cal*K/mole)
1	0.23	21.2	-17.6	-59.79
2	1.1	-5.3	-9.7	-36.22

Table E.3 Secondary structure thermodynamic properties for the test sequences [E.1].

The resulting Gibbs free energy and melting temperatures for the secondary structures of the test sequences indicates that they do not occur spontaneously. Ideally, this is optimal as this indicates that the formation of secondary structures is not a factor that will affect their function during in-lab experiments.

4) NCBI Blast Analysis

To verify that the sequence selected is part of the intended CYP2C19 cytochrome, NCBI blast was performed to check the matchings of sequences within *Homo sapiens*. Several matches were indicated by the NCBI blast with a 100% query cover and max score of 34.2 for the intended P450 CYP2C19 gene. This was done by testing the target sequence and results are shown in the following figure:

Sequences producing significant alignments									Download	Select columns	Show 100	?
		Description	Scientific Name	Max Score	Total Score	Query Cover	E value	Per. Ident	Acc. Len	Accession		
<input checked="" type="checkbox"/>	select all	5 sequences selected										
<input checked="" type="checkbox"/>		Homo sapiens isolate P68 cytochrome P450 (CYP2C19) gene_ exon 5 and partial cds	Homo sapiens	34.2	34.2	100%	155	100.00%	177	gi 1267712140 KY046734.1		
<input checked="" type="checkbox"/>		Homo sapiens isolate P58 cytochrome P450 (CYP2C19) gene_ exon 5 and partial cds	Homo sapiens	34.2	34.2	100%	155	100.00%	177	gi 1267708507 KY823015.1		
<input checked="" type="checkbox"/>		Homo sapiens isolate P8 cytochrome P450 (CYP2C19) gene_ exon 5 and partial cds	Homo sapiens	34.2	34.2	100%	155	100.00%	177	gi 1267707401 KY823013.1		
<input checked="" type="checkbox"/>		Homo sapiens isolate NA24385 chromosome 19	Homo sapiens	32.2	32.2	94%	614	100.00%	61317360	gi 2634424565 CP139524.1		
<input checked="" type="checkbox"/>		Homo sapiens isolate NA24385 chromosome 19	Homo sapiens	32.2	32.2	94%	614	100.00%	61355730	gi 2634358189 CP139547.1		

Figure E.8 NCBI Blast of target sequence showing matching results with intended gene [E.1].

5) Homo/Hetero-dimer Analysis

The following details the top three results of the homo-dimer analysis for the HPP and test sequences. This analysed the binding capabilities of each strand to another identical strand. Ideally, all Gibbs free energy values for homo-dimer analysis were significantly lower than the complete/partial hybridization of the sequences to their complementary portions of the HPP loop.

Additionally, the hetero-dimer analysis for the full hybridization of the target sequence is -33.39 kCal/mol whereas the partial hybridization for the mismatch sequences is -31.44 kCal/mol and -27.19 kCal/mol. This ensures that the likelihood of the mismatches binding to the HPP is less than the full hybridization. Additionally, since the mismatch-1 base swap is at the 3' end of the strand, it offers the maximum Gibbs free energy analysis any singular mismatch within the 17 base length sequence. This provides assurance that if its signal generation is under the target sequence, any swap along the sequence length will also have a signal generation under the target sequence.

Table E.4 Top 3 homo-dimer analysis for HPP and target sequences and hetero-dimer analysis between HPP and target sequences [E.1].

Sequence	Base Pairs	Gibbs free energy (kCal/mol)
HPP #1	6	-14.91
HPP #2	4	-9.89
HPP #3	4	-9.89
Target Sequence Hetero	17	-33.39
Target Sequence #1	2	-3.07
Target Sequence #2	2	-3.07
Target Sequence #3	2	-3.07
Mismatch-1 Hetero	16	-31.44

Mismatch-1 #1	2	-3.07
Mismatch-1 #2	2	-3.07
Mismatch-1 #3	2	-3.07
Mismatch-2 Hetero	13	-27.19
Mismatch-2 #1	2	-3.07
Mismatch-2 #2	2	-3.07
Mismatch-2 #3	2	-3.07

E.2 Electrochemical Electron Transfer System

E.2.1 Lineweaver-Burk

The signal amplification method that involved the enzymatic redox reaction between three main components:

- The enzyme Horseradish Peroxidase (HRP)
- The oxidizing agent hydrogen peroxide (H_2O_2)
- The substrate tetramethylbenzidine (TMB)

In the presence of HRP, TMB undergoes oxidation by H_2O_2 , resulting in the production of a blue TMB diimine product and water byproduct. Thus, to understand how the HRP enzyme interacts with TMB and H_2O_2 , the Lineweaver-Burk plots were simulated by holding each variable constant. The Michaelis constant values used for the simulation were $K_m_{TMB} = 0.5\text{mM}$, $K_m_{H_2O_2} = 3.7\text{mM}$ and $V_{max} = 0.1\mu\text{M/s}$ referenced from [EA.1]. A hypothetical HRP concentration of 0.75 was considered for the calculations.

Holding H_2O_2 at a constant concentration of 10mM, the corresponding reaction rates were calculated for the TMB substrate concentrations ranging from 0.1 to 10mM, using the Michaelis-Menten kinetics formulas discussed in Appendix B. Thus, the resulting Lineweaver-Burk plot of TMB concentration is shown in Figure E.9.

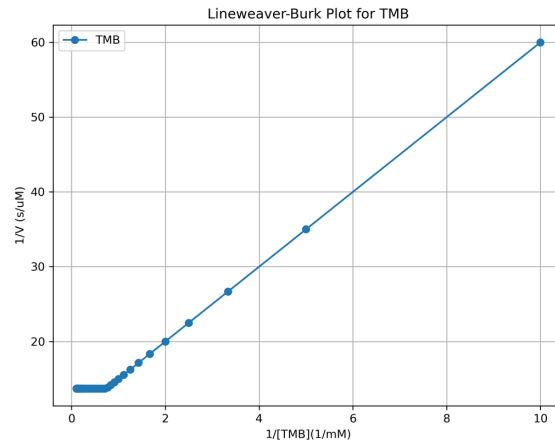


Figure E.9. Lineweaver-Burk plot of TMB concentration

Holding TMB at a constant concentration of 0.2mM, the corresponding reaction rates were calculated for the H_2O_2 concentrations ranging from 0.1 to 10mM, using the Michaelis-Menten kinetics formulas discussed in Appendix B. Thus, the resulting Lineweaver-Burk plot of H_2O_2 concentration is shown in Figure E.10.

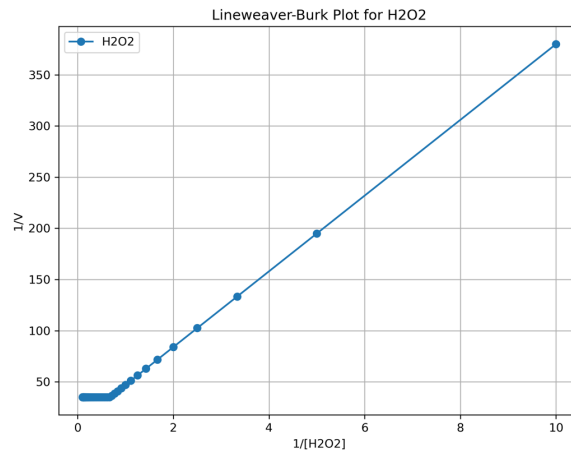


Figure E.10. Lineweaver-Burk plot of H_2O_2 concentration

Since both Lineweaver-Burk plots have a linear trend, they suggest that the reaction between TMB and H₂O₂ in the presence of HRP follow the Michaelis-Menten kinetics. The resulting slopes for each of the Lineweaver-Burk plots are as follows:

- Slope for TMB: 4.47

- Slope for H₂O₂: 33.50

A steeper slope suggests a lower Vmax and higher Km which is associated with a slower reaction and lower affinity to the enzyme. On the other hand, a flatter slope represents higher Vmax and lower Km indicating a faster reaction and higher affinity to the enzyme. This analysis demonstrated that the TMB substrate drives the faster reaction and serves as the main catalyst. Thus, the simulated concentrations were selected for the experimental protocols.

E.3 Capture Mechanism Coverage on the Electrode

E.3.1 Theoretical Coverage Calculation and Cyclic Voltammetry Curves

A volume of 20uL of 10 mM of MCH solution and a volume of 20uL of 1μM of HPP was dropped cast in the working electrode's surface. This approximately represents 20pmol of HPP and 200nmol of MCH; therefore, the total amount of SAM used to functionalize the working electrode was 200.02 nmol or 2.0002e-7 mol. The diameter of the working electrode was 2 mm. These values were used to estimate the SAM theoretical coverage value.

$$\text{Theoretical Coverage} = \frac{\text{Amount of SAM [mol]}}{\text{Electrode Surface Area}[\text{mm}^2]}$$

$$\text{Theoretical Coverage} = \frac{2.0002e - 7 [\text{mol}]}{\pi * r^2 [\text{mm}^2]} = \frac{2.0002e - 7 [\text{mol}]}{\pi * (2)^2 [\text{mm}^2]}$$

$$\text{Theoretical Coverage} = 1.5917 * 10^{-8} \left[\frac{\text{mol}}{\text{mm}^2} \right]$$

This theoretical coverage value represents the amount of SAM per unit area that was estimated to cover the working electrode's surface. This value helped us to understand how densely the SAM molecule was packed on the electrode surface.

Cyclic Voltammetry measurements were taken before (bare gold electrode) and after the deposition of the SAM layer, after MCH and HPP incubation, to verify its formation. Figure E9 represents the CV curves of the bare gold electrode and the electrode after deposition of SAM/HPP.

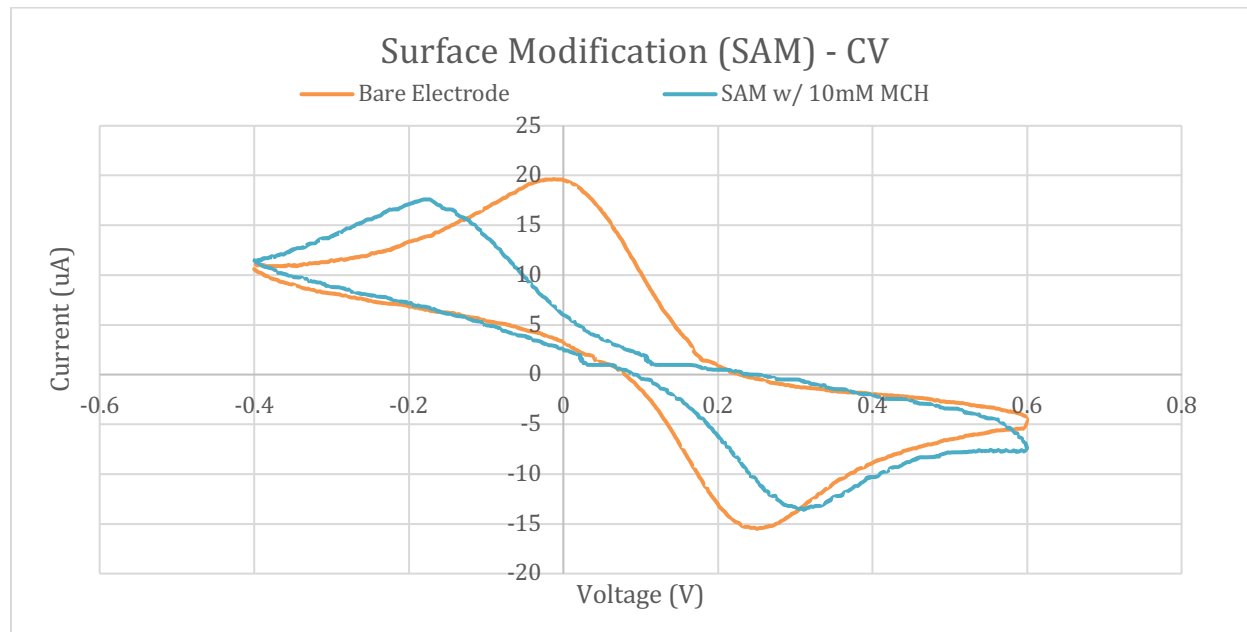


Figure E9. CV curve measured during characterization of SAM layer

From the CV curve of the bare electrode, a maximum current peak was found at 19.5 μ A. After the SAM was deposited and incubated on the electrode, the CV measurement showed a decrease in the maximum current peak to 17.6 μ A. This decrease was expected as the SAM layer hinders the electron transfer.

$$\text{Surface Coverage} = 1 - \left(\frac{Q_{\text{SAM}}}{Q_{\text{bare electrode}}} \right), \text{ where } Q \text{ represents the charge}$$

$$\text{Surface Coverage} = 1 - \left(\frac{17.6 \text{ } \mu\text{A}}{19.5 \text{ } \mu\text{A}} \right)$$

$$\text{Surface Coverage} = 0.097 = 9.7\%$$

The calculated surface coverage yielded a value of 0.097 which suggested that about 9.7% of the electrode surface area is no longer accessible for any electrochemical reaction after SAM deposition. The 9.7% does not directly represent the physical coverage but rather the reduction in electrochemical activity, proving that the SAM layer is forming a barrier that inhibits the flow of electrons between the electrode and the solution [E.2]. A reduction to 9.7% of the original current indicated that the SAM is well-formed and is covering the electrode's surface.

E.3.2 Spectroscopy and Beer's Lamber Law

UV-VIS spectroscopy was used to calculate the concentration of HRP-streptavidin. The HRP-Streptavidin material ordered for experiments came in a liquid format and had a concentration of 4000x. Thus, spectroscopy was selected to determine the range of concentration of HRP to be tested with the biosensor. Beer's Lamber Law indicates a linear relationship between the concentration of an absorbing species in solution and the magnitude of absorption of light at a specific wavelength. Higher concentrations saturate the absorption of light and do not follow the Beet-Lambert law [E.3]. Thus, the working range of concentration of HRP-Streptavidin that followed a linear relationship with the absorbance readings were selected for experiments as seen in Figure E.10. The concentration values were calculated following the formula discussed in Appendix B and shown in Table E.5.

Table E.5. UV-Vis absorbance related to concentration and dilution factor of HRP-STV.

HRP-STV dilution factor	Absorbance	Concentration
1:20	0.043	1.1685
1:25	0.039	1.0598
1:30	0.028	0.7609
1:50	0.016	0.4348

1:100	0.006	0.163
-------	-------	-------

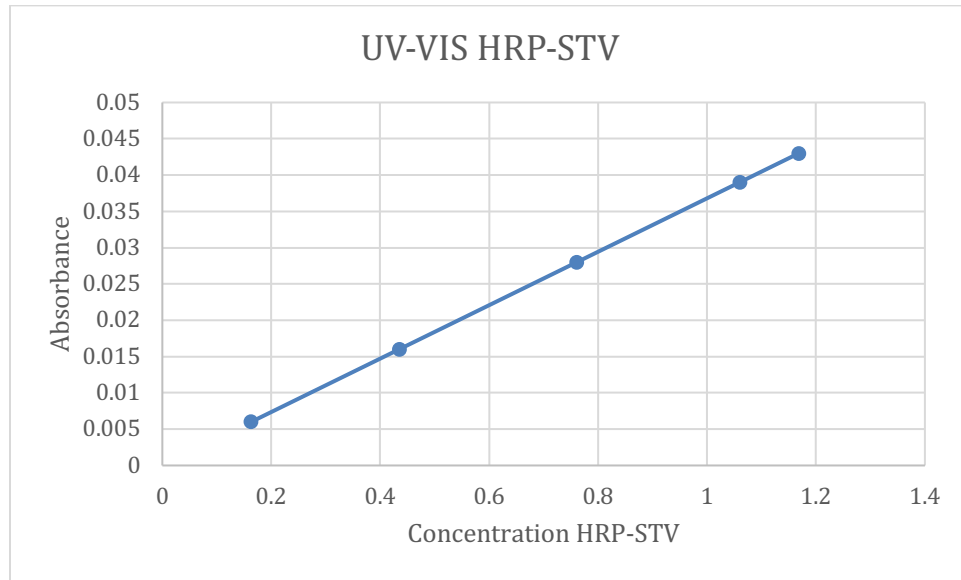


Figure E.10. Linear relationship between absorbance and concentration of HRP-STV.

E.3.3 Electrochemical Impedance Spectroscopy (EIS)

EIS measurements were taken for SAMs of: 1) 1uM hairpin probe (HPP) incubated during 1.5h and 10mM MCH incubated for 20mins, and 2) 1uM HPP incubated during 1h and 50uM MCH incubated for 1h. In both cases, there was an increase in the curvature of the Nyquist plot when compared to the bare gold electrode. However, with the second formulation of 50uM MCH a less saturated surface was expected, and so, the curvature should have been smaller than that of 10mM MCH incubated for 20mins, see Figure E.11. These results can be attributed to fabrication differences and the age of the materials, particularly that of the hairpin probes which had not been resuspended before the incubation, or the presence of contaminants.

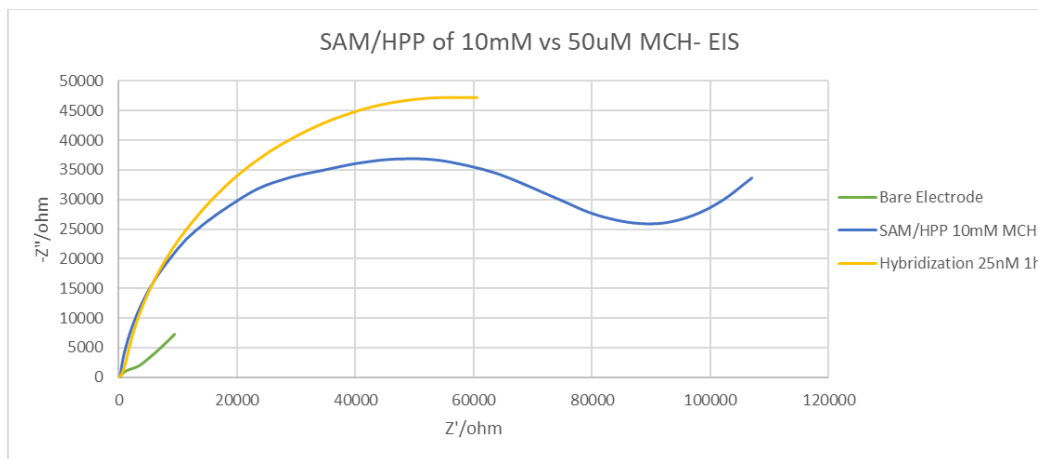


Figure E.11. EIS measurements comparing MCH concentrations and bare electrode

E.3.4 Scanning Electron Microscopy (SEM)

SEM images were taken for two samples that were spin-coated with an AuNPs solution with initial effective diameter of 47.08.35 nm and a polydispersity of 0.260. The AuNPs were spin-coated onto the sample a month after the AuNPs solution was synthesized. As shown in Figure E.12, the SEM image shows a non-uniform, granular landscape which can represent clusters and particle aggregations.

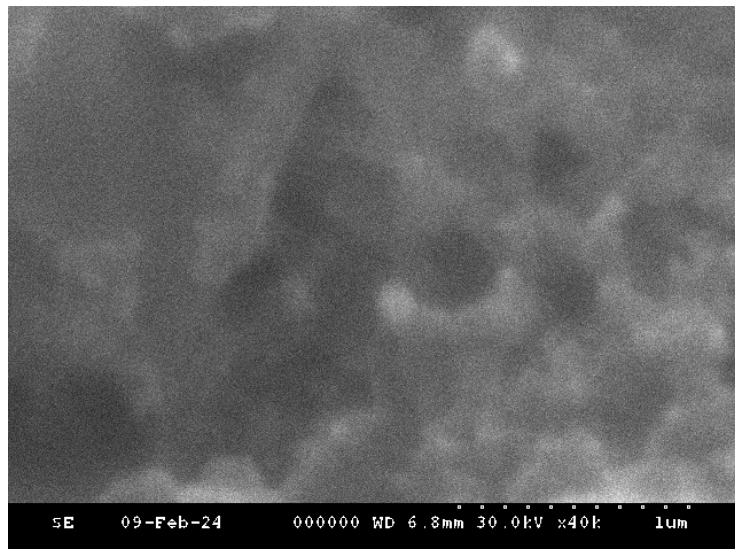


Figure E.12. SEM image of AuNPs

E.3.5 Dynamic Light Scattering (DLS)

DLS was used to determine the particle size of AuNPs. Two DLS measurements were performed on different days to identify any aggregation of the AuNPs. The first measurement was taken the same day the AuNPs were synthesized, and the second measurement was taken a month after the synthesis of the AuNPs. The DLS results are presented in Table E.5.

The analysis revealed an increase in the particle size from 47 nm to 66 nm, which could adversely affect the stability of the GeneDetek sensor. Also, the DLS results indicated the presence of contaminants, highlighting potential quality issues with the AuNPs batch.

Table E.5. Characterization results from DLS and UV/Vis

DLS (Synthesis Day)	DLS (After a month)
Eff Diam (nm) = 47.08	Eff Diam (nm) = 66.00
Polydispersity = 0.260	Polydispersity = 0.354

References:

- [E.1] “OligoAnalyzer,” Accessed on: Jan. 4, 2024. [Online]. Available: <https://www.idtdna.com/calc/analyzer>
- [E.2] A. J. Bard, L. R. Faulkner, and H. S. White, *Electrochemical Methods: Fundamentals and Applications*. Hoboken, NJ, USA: John Wiley & Sons, Inc, 2022.
- [E.3] Cajigas, S., Alzate, D., Fernández, M., Muskus, C., & Orozco, J. (2022). Electrochemical genosensor for the specific detection of SARS-CoV-2. In *Talanta* (Vol. 245, p. 123482). Elsevier BV. <https://doi.org/10.1016/j.talanta.2022.123482>

Appendix F: Prototype Test / Measurement Data

Test results of the different iterations to reach the final working prototype discussed in section 2.4 are included in this appendix. The format follows the same breakdown of information as the test plan, based on the customer requirements.

F.1 Primary Requirements

1) Specific to polymorphism CYP2C19*2

The technique used to compare the results between blank, 20nM of target DNA, 20nM of mismatch-1 and 20nM of mismatch-2 was DPV as seen in Figure F.1. The blank measurement was considered an offset and mismatch-2 current peak resulted to be above the target DNA current peak which was unexpected. However, mismatch-1 current peak is below the target DNA current peak as expected.

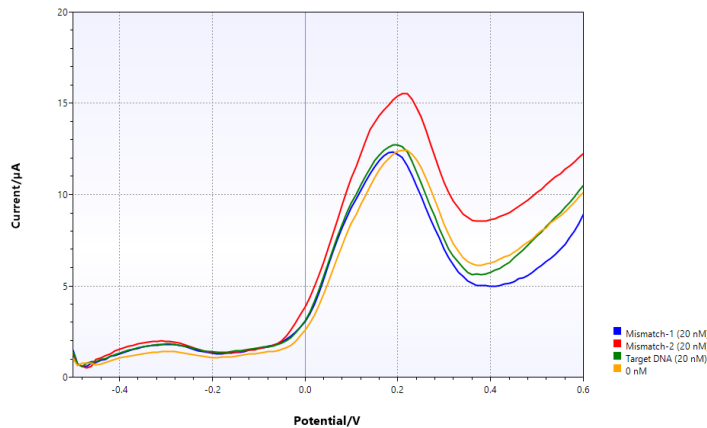


Figure F. 1. DPV measurement of blank, target DNA, mismatch-1 and mismatch-2 at 20nM concentration

2) Sensitive to low concentrations

2.1) Signal-to-noise ratio (SNR)

All information was covered in Section 2.4. in the main body.

2.2) Calibration Curve

A total of four calibration curves had been developed, each changing different variables to optimize our biosensor's response. The variables are:

- **MCH concentration for SAM layer**

Cyclic Voltammetry (CV) and Electrochemical Impedance (EIS) measurements were taken before and after the deposition to verify its formation. The concentration of HPP was kept at 1uM in all experiments, and the concentrations of MCH were tested at 10mM (incubated for 20 mins) and 50uM (incubated for 1h). Furthermore, surface coverage was assessed through the Randles–Sevcik equation of CV performed at different scan rates. The plots corresponding to these variables can be seen in Figure F.2 and Figure F.3 respectively.

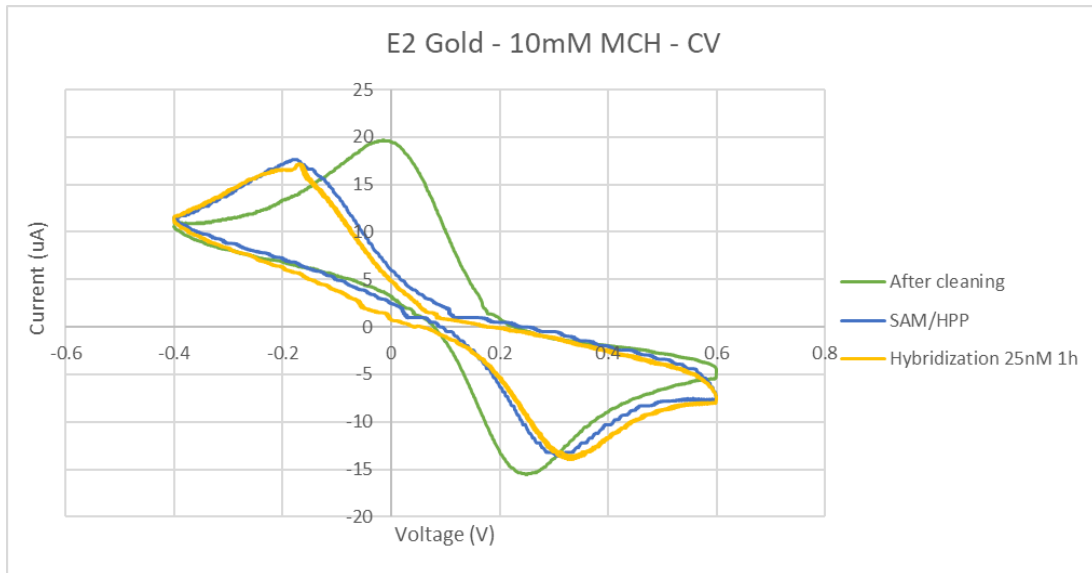


Figure F. 2. CV curves of sensor fabrication after acid cleaning, SAM/HPP deposition using 10mM MCH and 1hour hybridization of 25nM of target DNA.

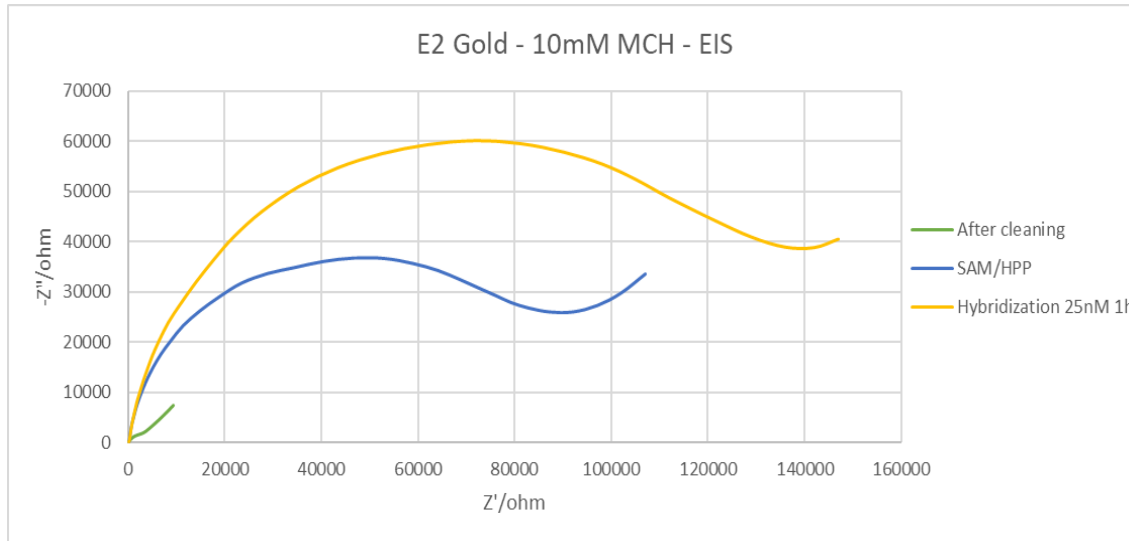


Figure F. 3. EIS curves of sensor fabrication after acid cleaning, SAM/HPP deposition using 10mM MCH and 1hour hybridization of 25nM of target DNA.

A decrease in the current peak and an increase in impedance signal were expected, so the 10mM MCH recipe was considered successful and calibration curve data was collected. A linear

trend was expected for CV and chronoamperometric measurements; however, only CV was consistent as chronoamperometric readings needed further tuning to find the potential with highest response. The second approach, 50uM MCH, showed the expected increase of curvature in the Nyquist plot compared to the bare electrode, and a decrease in CV signal similar to 10mM MCH so it was considered a successful SAM formation.

The measurements for CV and chronoamperometry were more consistent for the 10mM MCH approach as seen in Figure F. 4, so subsequent data was collected with that SAM layer.

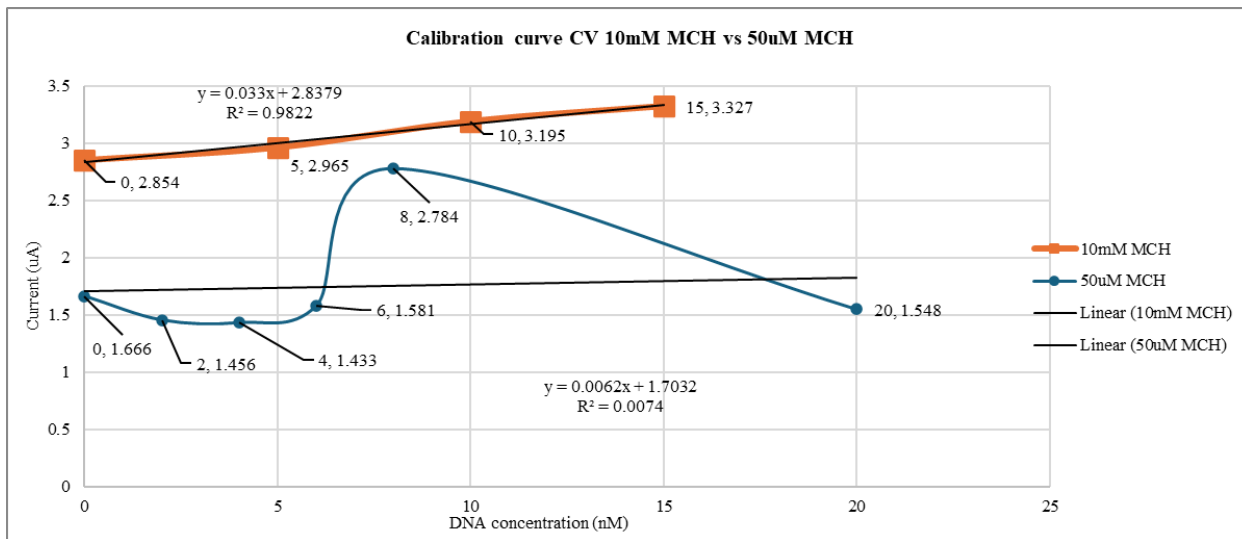


Figure F. 4. Calibration curve comparison between SAM using 10mM vs 50uM MCH.

- HRP dilution factor

The stock solution of HRP-Streptavidin had a concentration of 4000x. An initial dilution of 1:4000 in 1xPBS was prepared and tested under UV-VIS. However, no signal was obtained, and the dilution factor was adapted to 1:100 in 1xPBS. A purple coloration was observed in the HRP-Streptavidin buffer, suggesting instability of the enzyme conjugate in PBS. Thus, an enzyme dilution buffer containing BSA was used instead of 1xPBS.

To optimize the HRP concentration ideal for the system, a UV-VIS characterization at different dilution factors was performed as seen in Figure F.5. The target dilution factor was the maximum concentration that followed the Beer Lambert law, meaning the point of transition from a linear to a logarithmic trend. Thus, a dilution factor of 1:30 is suggested as optimal as seen in Table F.1.

Table F. 1. UV VIS absorbance values from different HRP dilution factors and their respective concentrations

Dilution factor	Volume HRP-STV(uL)	Absorbance	Concentration
1:20	75	0.043	1.1685
1:25	60	0.039	1.0598
1:30	50	0.028	0.7609
1:50	30	0.016	0.4348
1:100	15	0.006	0.163

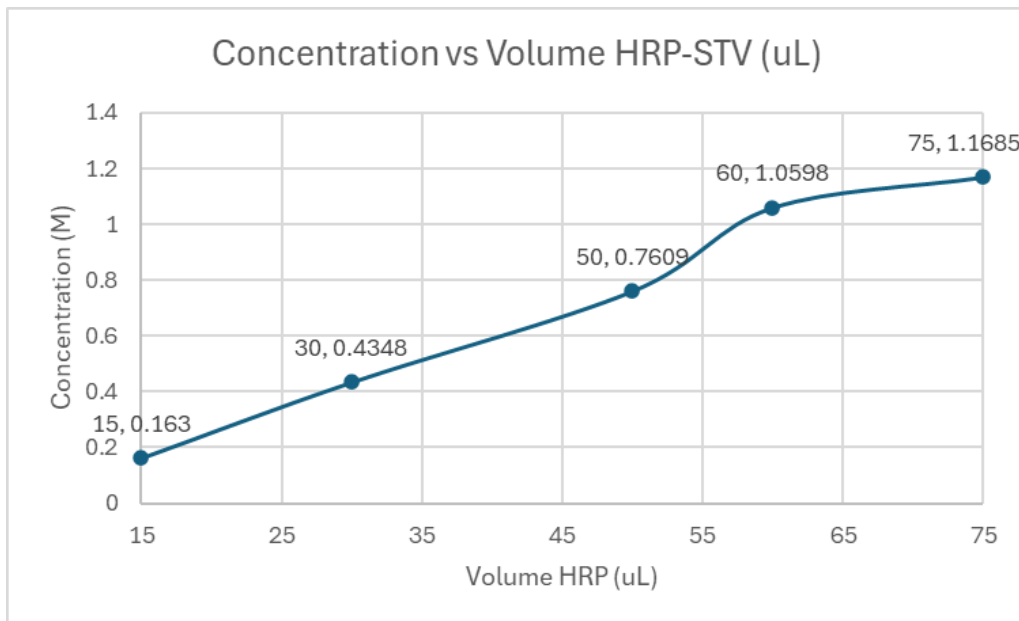


Figure F. 5. Concentration vs Volume of HRP-Streptavidin

- H₂O₂ concentration

The reference paper suggested a concentration of 0.2mM TMB/1mM H₂O₂ to obtain an upward linear calibration curve. However, using a concentration of 1mM resulted in a negative slope as opposed to 10mM which gave a positive slope as seen in Figure F.6. The calibration curves used the amperometry data obtained at a fixed potential of 0.4V. Therefore, a concentration of 10mM H₂O₂ was used in the detection buffer for the working prototype.

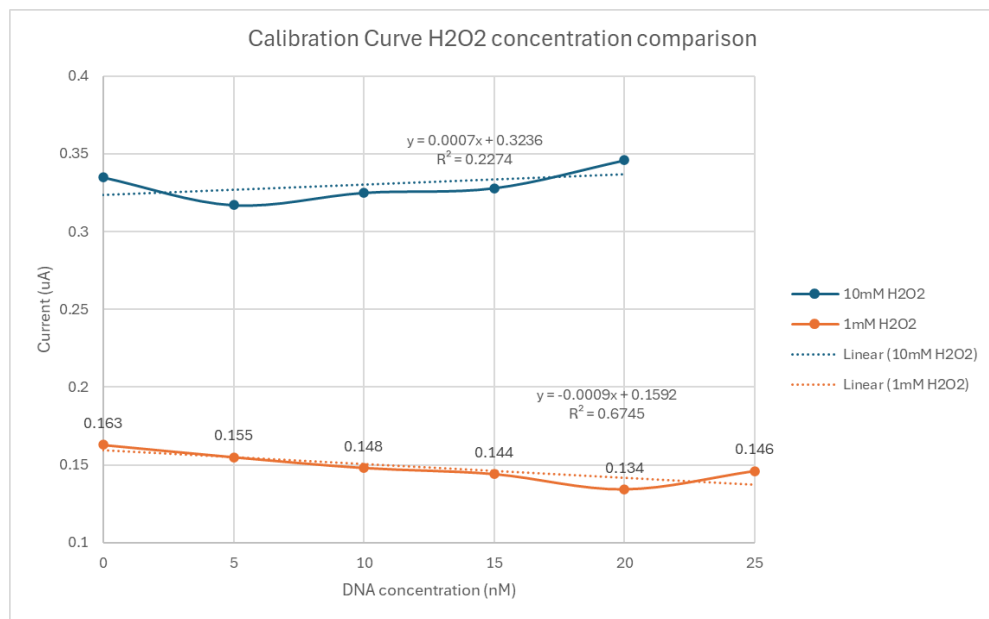


Figure F. 6. Calibration curves at different H₂O₂ concentrations: 10mM vs 1Mm.

- Final Calibration Curve

The CV curves that correspond to some of the values in the calibration curve can be seen in Figure F. 7. The CV oxidation peaks at 0.3V were considered for the calibration curve.

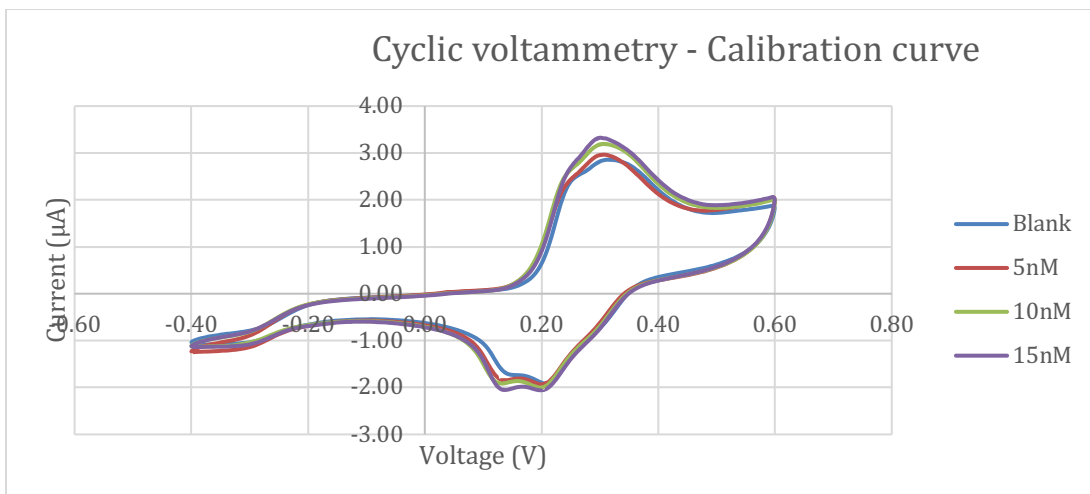


Figure F. 7. CV curves of calibration curve values.

2.3) Limit of Detection (LOD)

All information was covered in Section 2.4. in the main body.

2.4) Linearity

All information was covered in Section 2.4. in the main body.

3) Target to saliva sampling

All information was covered in Section 2.4. in the main body.

4) Portability & Ergonomics

All information was covered in Section 2.4. in the main body.

F.2 Secondary Requirements

1) Rapid Testing and Detection

1.1) Hybridization Time

The one-hour incubation time was determined by running measurements at different time intervals following the deposition of the target DNA onto the electrode. For a concentration of 25

nM of target DNA, the measurements were conducted after 20 min (Figure F.8), 45 min (Figure F. 9), and 1 hour (Figure F. 10). For 5nM of target DNA, measurements were taken only after 45 min (Figure F. 11).

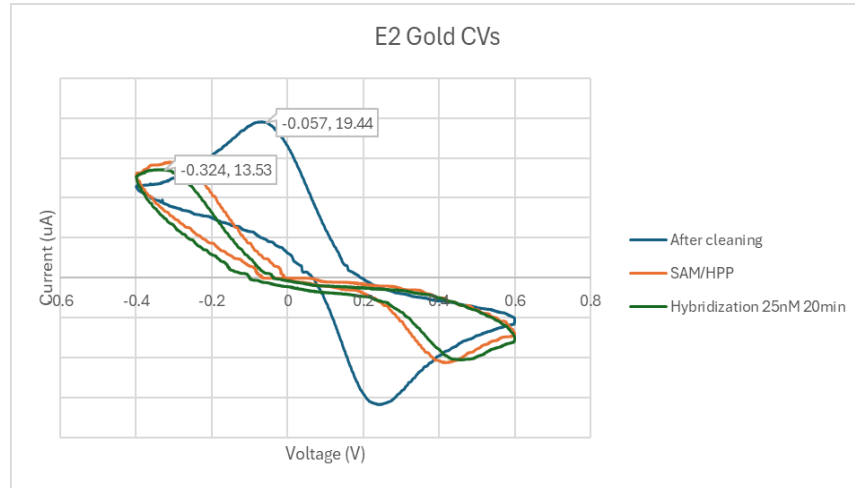


Figure F.8 8. Hybridization with 25nM target DNA for 20 min.

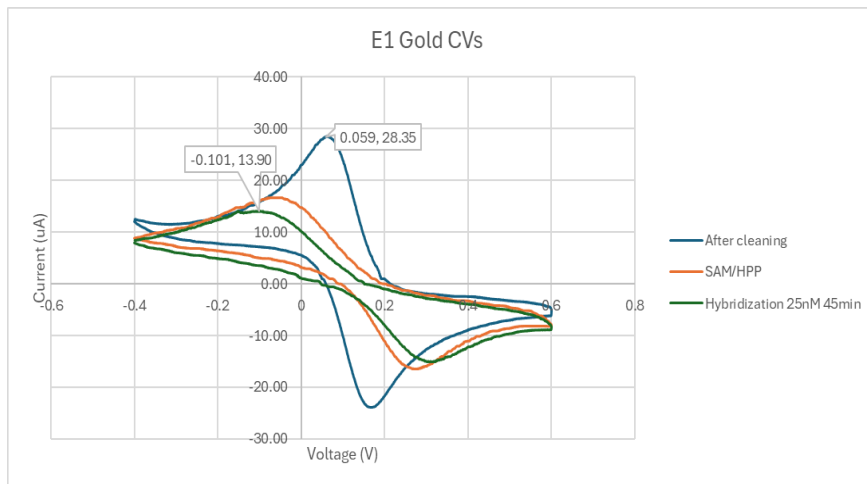


Figure F.9 9. Hybridization with 25nM target DNA for 45 min.

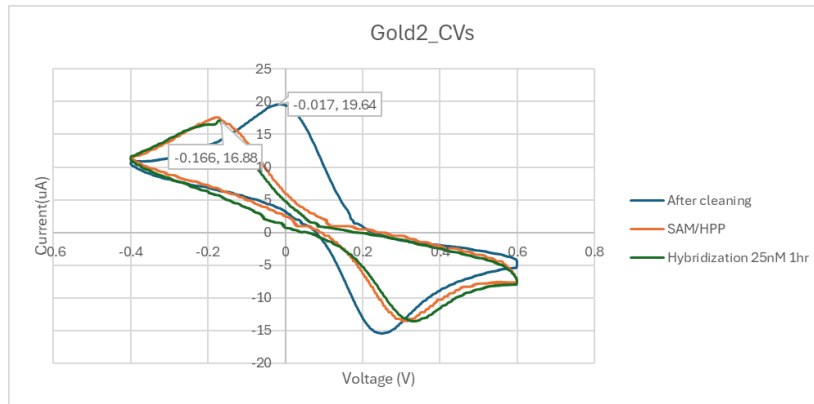


Figure F. 1010. Hybridization with 25nM target DNA for 1 hour.

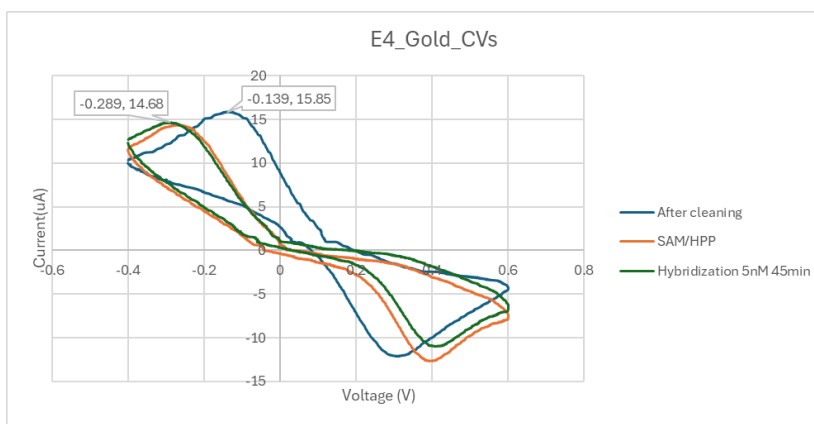


Figure F. 1111. Hybridization with 5nM target DNA for 45 min.

The CV curve can portray two behaviors: 1) a shift in the CV curve indicates a change in diffusivity (doble layer change) that can be caused by the presence of layers in the surface and 2) a change in peak current depending on the electron transfer efficiency of the electrode surface. The shift in the CV curve is evident in all tests as the same SAM/HPP layer was deposited. However, the peak current increases with increasing incubation time for hybridization. Thus, the hybridization time of the smallest difference of 2.76 between the bare electrode and hybridization peak current was selected as seen in Table F.2. This corresponded to one-hour hybridization time. A concentration of 5nM was included to corroborate the results.

Table F. 2. CV oxidation current peaks of hybridization measurements.

		Oxidation current peaks (uA)			
		25 nM			5 nM
		E1 (45 min)	E2 (20 min)	E3 (1hr)	E4 (45 min)
Bare electrode		28.35	19.44	19.64	15.85
Hybridization		13.90	13.53	16.88	14.68
Subtraction		14.45	5.91	2.76	1.17
Ratio		0.4903	0.695988	0.85947	0.9261

1.2) Reaction Time Assessment

All information was covered in Section 2.4. in the main body.

2) Cross-Reactivity

The ANOVA statistical test was used to determine the statistical relevance of the difference between the experimental data of the calibration curve and the linear regression. The results can be found in Figure F.12. The resultant p-value is less than 0.05, thus indicating the difference is not statistically significant and it is considered a pass.

ANOVA

		DF	Sum of Squares	Mean Square	F Value	Prob>F
CURRENT	Model	1	1.84103	1.84103	25.05677	0.03767
	Error	2	0.14695	0.07347		
	Total	3	1.98798			

At the 0.05 level, the slope is significantly different from zero.

Figure F.12 12. ANOVA test results of calibration curve.

However, due to the lack of electrodes, it was not possible to gather information to test hybridization without HRP and run a 2-side ANOVA as initially planned.

3) Small Sample Volume Compatibility

All information was covered in Section 2.4. in the main body.

4) Usability and User-Friendly

All information was covered in Section 2.4. in the main body.

Overall, the presented results from the comprehensive test plan conclusively demonstrate that the customer requirements were met as seen in Table F.3.

Table F.33. Side-by-side comparison of the Test Results versus the Customer Requirements.

Primary requirements	Test quantifiers	Pass/fail criteria	Pass/Fail Results
1) Specific to polymorphism CYP2C19*2	Compare signal ratios of target DNA to mismatch DNA	3:1 target sequence to non-cognate sequence 2:1 target sequence to 1- and 2-mismatch	Target:Blank = 9.776:1 ✓ Target:M1 = 2.069 :1 ✓ Target:M2 = 0.5308 :1 ✗
2) Sensitive to low concentrations	Calibration curve/linearity SNR LOD	Linear calibration curve SNR is at least three times higher than the background noise Value <10nM or >3SD	Linear ✓ SNR = 33.27 ✓ Noise = 0.10 uA ✓ LOD = 4.173 nM ✓
3) Target to saliva sampling	Compare the signal response of target DNA in artificial saliva to the signal response of target DNA in Phosphate buffer saline	Total error within tolerance of 10%	Ongoing
4) Test for Portability and Ergonomics	Compare the design's dimensions against the threshold values	<20 g, <20 cm, <20 cm	The final dimensions of the GeneDetek biosensor are: Weight = 10.68g ✓ Length = 3.2 cm ✓ Width = 4.0 cm ✓ Height = 8 mm (not considered in the requirements)
Secondary requirements	-		
1) Rapid Testing and Detection	Hybridization time Reaction Time Assessment	Perform fluorescence measurements at different time intervals, time should be < 24h. Time to: 1) collect a saliva sample, 2) prepare the saliva sample, 3) place the specimen on the biosensor and obtain a signal, and 4) analyze the results; is <24hr	Instead of fluorescence measurements, CV and Impedance measurements were performed at different times to determine hybridization. Hybridization time: 1 hr ✓ Total time: ~ 7 hours ✓

2) Cross-Reactivity (with/without HRP)	Conduct test of signal ratios with target sequence and non-cognate sequences with and without contamination	Signal ratios of 2:1 between the target sequence and non-cognate sequences	ongoing
3) Small Sample Volume Compatibility	Consistent with the LOD Test results	Concentration below 10nM	LOD = 5.561 nM <input checked="" type="checkbox"/>
4) Usability and User-Friendly	Usability test	The user interface must be easy to follow.	User friendly <input checked="" type="checkbox"/>

Appendix G: FYDP Resources

Budget

Table G1. Budget

Category	Item	Unit cost (\$)	#	Total Cost
Hairpin-loop Probe and DNA	Hairpin Loop Probe	176.85	1	176.85
	Synthetic DNA	84.1	3	252.3
Materials	Artificial Saliva	220	1	220
	HRP-Streptavidin	107	1	107
	Electrodes	4.74	68	322.32
Equipment	SEM	50	1	50
	Poster	43.28	1	43.28
Total Spent				1171.75
Total Remaining				228.25

External Awards

Our team participated and won the Esch Pitch Competition, receiving a financial award of \$5000 aiming to support creative and entrepreneurial students in the pursuit of research and development.

Lab Equipment Used

For running and validating the experiments, we used equipment from the NE Undergrad Labs as well as from our consultant's lab which is Tang's Lab. To print the encasing of the biosensor, 3D printers from the Rapid Prototype Center in E7 were used.

Table G2. Lab Equipment Used

Equipment in NE UG labs	Tang's Lab	Rapid Prototype Center
Spin Coater	Potentiostat	3D Printer
SEM	Fume Hood	
UV/Vis	Standard Laboratory Equipment	
DLS		

Team Member's Activities and Contributions to the FYDP

Team member's	A brief articulation of the specific activity or contribution made by the team member	Activity dates	No of hours	Signature
Andrea	Hybridization time testing	01/03/2024	6	AP
	Buffer prep	04/03/2024	2	AP
	HRP protocol tunning	05/03/2024	8	AP
	1st Calibration curve protocol	06/03/2024	8	AP
	2nd Calibration curve protocol	08/03/2024	8	AP
	3rd Calibration curve (failed) protocol	12/03/2024	8	AP
	50uM vs 10mM MCH blank measurement	13/03/2024	3	AP
	Replication of 1st Calibration curve protocol	14/03/2024	8	AP
	Test data obtained from the design prototype	14/03/2024	2	AP
	Demo prep	15/03/2024	2	AP
	Workflow in Biorender for Poster	16/03/2024	3	AP
	Poster prep	17/03/2024	3	AP
	Buffer prep	18/03/2024	6	AP
	Electrode reusability literature review	18/03/2024	2	AP
	Commercial electrodes saliva testing	20/03/2024	10	AP
	1mM MCH test and saliva testing	21/03/2024	6	AP
	Seminar presentation prep	21/03/2024	3	AP
	Norman Esch prep	27/03/2024	4	AP
	Prototype Sign-off prep	03/04/2024	1	AP
	Final Report drafting	04-08/04/2024	10	AP
Karla	SAM Deposition + Hybridization Test Lab Support	01/03/2024	4	KC
	Chip Design Brainstorming	01/03/2024	1.5	KC
	Chip Design Solidworks	02/03/2024	4	KC
	3D Print Design 1	03/03/2024	3.5	KC
	Esch Award Presentation	06/03/2024	3	KC
	3D Print Design 2 (Modified Design + Troubleshooting printer)	06/03/2024	5	KC
	Esch Award Presentation - Slides + Recording	07/03/2024	12	KC
	3D Print Design 2	07/03/2024	2	KC

	Software Developement (Main Functions)	08/03/2024	10	KC
	Calibration curve 2 Lab Support	08/03/2024	3	KC
	Calibration curve 3 Lab Support	12/03/2024	3	KC
	Software Developement (Streamlit App)	13/03/2024	10	KC
	Replication of 1st calibration curve Lab Support	14/03/2024	3	KC
	Software 1st working prototype	15/03/2024	2	KC
	Results Document for Demo	15/03/2024	2	KC
	Poster Prep	15/03/2024	4	KC
	Poster Design	17/03/2024	2	KC
	Final Software (App + Report)	17/03/2024	6	KC
	Demo Video Seminar	19/03/2024	3	KC
	Final Demo Video Seminar	21/03/2024	5	KC
	Seminar Presentation prep	21/03/2024	3	KC
	Norman Award Animation	26/03/2024	3	KC
	Norman Esch Prep	27/03/2024	4	KC
	Final Reporting Darfting	08/04/2024	12	KC
Nube	Lab activities support	01/03/2024	2	NT
	Literature Review: SAM layer	10/03/2024	4	NT
	SAM deposition, 50uM MCH protocol	11/03/2024	11	NT
	Calibration Curve, support	08/03/2024	2	NT
	Calibration Curve + Mismatches, support	12/03/2024	2	NT
	Demo prep (Test data, customer requirements)	15/03/2024	4	NT
	FYDP Poster	17/03/2024	4	NT
	Cleaning SPE Protocol	18/03/2024	3	NT
	FYDP Seminar Prep	21/03/2024	5	NT
	FYDP Seminar & Symposium	22/03/2024	6	NT
	Esch Competition Prep	27/03/2024	5	NT
	FYDP Report	08/04/2024	12	NT
Sara	Lab: Electrodes + HRP Protocol	05/03/2024	4	ST
	Lab: Calibration Curve Protocol (0-25 nM)	06/03/2024	8	ST
	Lab: Calibration Curve Protocol (0-25 nM) + Mismatches	08/03/2024	8	ST

	Lab prep	11/03/2024	2	ST
	Lab: Calibration Curve + Mismatches	12/03/2024	8	ST
	Lab: New Blanks protocol	13/03/2024	4	ST
	PSTrace data analysis	13/03/2024	2	ST
	Literature Review: DNA Hybridization	13/03/2024	3	ST
	Lab: Calibration Curve	14/03/2024	7	ST
	PSTrace data analysis	16/03/2024	1	ST
	FYDP Poster	16-17/03/2024	4	ST
	Lab: Cleaning Commercial Electrodes Protocol	18/03/2024	2	ST
	FYDP Seminar	19/03/2024	6	ST
	Lab: Commercial Electrodes Calibration Curve with Saliva	20/03/2024	12	ST
	Lab: Commercial Electrodes with Saliva	21/03/2024	6	ST
	FYDP Seminar	21/03/2024	4	ST
	Esch Competition Questions Prep	27/03/2024	3	ST
	FYDP Report	5-8/04/2024	9	ST
Total hours: 366	Andrea Parra: 103	Karla Castro: 110	Nube Torres: 60	Sara Thompson: 93